Candida glabrata maintains two Hap1 homologs, Zcf27 and Zcf4, for distinct roles in ergosterol gene regulation to mediate sterol homeostasis under azole and hypoxic conditions

Debasmita Saha[1], Justin B. Gregor[1], Smriti Hoda[1], Katharine E. Eastman[1], Mindy Navarrete[1], Jennifer H. Wisecaver[1] and Scott D. Briggs[1,2#]

[1]*Department of Biochemistry and* [2]*Purdue University Institute for Cancer Research*

KEYWORDS: *Candida glabrata*, zinc cluster transcription factors, azole antifungal drugs, hypoxia, ergosterol pathway, *ERG11*, *ERG3,* Hap1, Zcf27, and Zcf4

Word count of abstract: 249 out of 250 max

[#]To whom correspondence should be addressed: Scott D. Briggs, Department of Biochemistry, Hansen Life Science Research Building, 201 S. University Street, West Lafayette, IN 47907, Phone: 765-494-0112, E-mail: sdbriggs@purdue.edu

ABSTRACT

Candida glabrata exhibits innate resistance to azole antifungal drugs but also has the propensity to rapidly develop clinical drug resistance. Azole drugs, which target Erg11, is one of the three major classes of antifungals used to treat *Candida* infections. Despite their widespread use, the mechanism controlling azole-induced *ERG* gene expression and drug resistance in *C. glabrata* has primarily revolved around Upc2 and/or Pdr1. In this study, we determined the function of two zinc cluster transcription factors, Zcf27 and Zcf4, as direct but distinct regulators of *ERG* genes. Our phylogenetic analysis revealed *C. glabrata* Zcf27 and Zcf4 as the closest homologs to *Saccharomyces cerevisiae* Hap1. Hap1 is a known zinc cluster transcription factor in *S. cerevisiae* in controlling *ERG* gene expression under aerobic and hypoxic conditions. Interestingly, when we deleted *HAP1* or *ZCF27* in either *S. cerevisiae* or *C. glabrata,* respectively, both deletion strains showed altered susceptibility to azole drugs, whereas the strain deleted for *ZCF4* did not exhibit azole susceptibility. We also determined that the increased azole susceptibility in a *zcf27Δ* strain is attributed to decreased azole-induced expression of *ERG* genes, resulting in decreased levels of total ergosterol. Surprisingly, Zcf4 protein expression is barely detected under aerobic conditions but is specifically induced under hypoxic conditions. However, under hypoxic conditions, Zcf4 but not Zcf27 was directly required for the repression of *ERG* genes. This study provides the first demonstration that Zcf27 and Zcf4 have evolved to serve distinct roles allowing *C. glabrata* to adapt to specific host and environmental conditions.

IMPORTANCE

Invasive and drug-resistant fungal infections pose a significant public health concern. *Candida glabrata*, a human fungal pathogen, is often difficult to treat due to its intrinsic resistance to azole antifungal drugs and its capacity to develop clinical drug resistance. Therefore, understanding the pathways that facilitate fungal growth and environmental

adaptation may lead to novel drug targets and/or more efficacious antifungal therapies. While the mechanisms of azole resistance in *Candida* species have been extensively studied, the roles of zinc cluster transcription factors, such as Zcf27 and Zcf4, in *C. glabrata* have remained largely unexplored until now. Our research shows that these factors play distinct yet crucial roles in regulating ergosterol homeostasis under azole drug treatment and oxygen-limiting growth conditions. These findings offer new insights into how this pathogen adapts to different environmental conditions and enhances our understanding of factors that alter drug susceptibility and/or resistance.

INTRODUCTION

Invasive and drug resistant fungal infections are significant public health issues and new estimates indicate that life-threatening fungal infections affect over 6.5 million people globally each year (1). Among these global invasive fungal infections, more than 70% are caused by invasive *Candida* species which include *Candida albicans* and other non- *albicans* (NAC) *Candida* species such as *C. glabrata*, *C. krusei*, *C. tropicalis*, and *C. parapsilosis* (2-5). Of the NAC species listed, *Candida glabrata* is considered the second or third most commonly isolated NAC *Candida* species, with *C. albicans* being the most commonly isolated (2, 4-6). The traditional genus *Candida* is a paraphyletic group, and *C. glabrata* is more closely related to *S. cerevisiae* than to other common human pathogens including *C. albicans* (7). The last common ancestor (LCA) of *C. glabrata* and *C. albicans* existed ~250 million year ago (Mya) whereas the LCA of *C. glabrata* and *S. cerevisiae* occurred ~50 Mya (8). *C. glabrata* is considered the major pathogenic species of the post-whole genome duplication (WGD) *Saccharomycetaceae* group, with immunosuppressed patients (e.g., those with diabetes mellitus, cancer, or organ transplants) and/or elderly patients being particularly susceptible to these infections (6, 9-12).

C. glabrata (*Cg*) is also a non-CTG clade *Candida* species that is known for its intrinsic resistance to azole drugs and ability to develop clinical azole drug resistance (7, 13, 14). Azole

drugs target and inhibit the enzyme lanosterol 14-α-demethylase (Erg11) which is an essential enzyme for the production of ergosterol in fungi (15-17). Mechanisms of acquiring clinical azole drug resistance have been extensively documented across *Candida* species and include mutations in *ERG11*, *ERG3*, *UPC2* and/or *PDR1* (14, 18-25). Among these genes, gain of function (GOF) mutations in the zinc cluster transcription factors Upc2 and Pdr1 result in increased expression of *ERG11* and/or the ABC drug transporter *CDR1,* respectively (24, 26-30). As for *C. glabrata* clinical drug resistant isolates, Pdr1 GOF mutations are considered the predominant cause for clinical drug resistance (28, 31).

In addition to Upc2 and Pdr1, several known and/or putative zinc cluster factors (Zcf) are critical transcriptional regulators involved in stress response in fungi and amoeba (32, 33). Interestingly, 17 of the 41 *C. glabrata ZCF* genes when deleted show enhanced azole susceptibility as indicated by MIC and/or plate-based growth assays (34). This observation underscores the importance and need to further investigate the role of these zinc cluster transcription factors in *C. glabrata*. However, with the exception of Upc2A (*CgZCF5*), Pdr1 (*CgZCF1*), Stb5 (*CgZCF24*), and Mar1 (*CgZCF4*), little research has been done to understand the mechanistic role of other *C. glabrata* Zcf proteins during azole treatment conditions and/or hypoxic growth (30, 35-39).

In this report, we show for the first time that *S. cerevisiae* (*Sc*) strains deleted for *HAP1* exhibit azole hypersusceptibility when compared to a FY2609 WT strain containing a WT copy of the *HAP1* gene. Interestingly, S288C strains, including the commonly used BY4741 and BY4742, exhibit similar azole susceptibility to *hap1Δ* strains due to a partially disrupted *hap1* gene by a *Ty1* element (*hap1-Ty1* mutant). Based on these observations, we hypothesized that deletion of *C. glabrata HAP1* homologs would also have a similar azole susceptible phenotype. Our phylogenetic analysis indicated that *C. glabrata* contains two proteins, Zcf27 and Zcf4, which are homologs of *S. cerevisiae* Hap1. However, only deletion of *C. glabrata ZCF27,* but not *ZCF4,* showed an azole hypersusceptible phenotype. Upon further investigation, we established

that altered azole susceptibility of the *zcf27Δ* strain is attributed to a decrease in azole-induced *ERG* gene expression, resulting in a subsequent reduction in total ergosterol levels. Moreover, azole hypersusceptibility of the *zcf27Δ* strain was alleviated when complemented with a plasmid expressing *ZCF27* or when exogenous ergosterol was introduced into the growth media, but not when the *AUS1* sterol transporter was deleted. Interestingly, unlike Zcf27, Zcf4 protein was nearly undetectable under both untreated and azole-treated conditions. However, under hypoxic conditions Zcf4 was highly induced, while the expression of Zcf27 remained unchanged. Moreover, the *zcf4Δ* strain showed a growth defect under hypoxic conditions while the *zcf27Δ* strain grew similar to *Cg*2001 WT. Additionally, our studies demonstrated that Zcf27 and Zcf4 can associate with promoters of *ERG* genes, and their enrichment at these sites is further enhanced upon azole treatment or hypoxic conditions, respectively. Overall, we have discovered that *C. glabrata* maintains two Hap1 homologs to regulate ergosterol homeostasis. Specifically, Zcf27 aids in facilitating azole-mediated gene activation, while Zcf4 mediates hypoxia-induced gene repression.

RESULTS

Hap1 alters azole susceptibility in *S. cerevisiae*.

In *S. cerevisiae*, there are three zinc cluster transcription factors Upc2, Ecm22 and Hap1 that are known to regulate the expression of ergosterol gene expression for sterol homeostasis (40-44). In addition, Upc2 and Ecm22 are also known to mediate azole susceptibility in *S. cerevisiae* (45, 46). However, until now, the role of Hap1 in altering azole susceptibility has not been determined. To test this hypothesis, the *hap1-Ty1* mutant was deleted in S288C strains BY4741 and FY2609 to generate BY4741 *hap1Δ* (this study) and FY2611 *hap1Δ* (40), respectively (see Supplemental Table S3). The indicated strains were tested for growth in liquid cultures and through serial-dilution spot assays with and without 16 µg/mL fluconazole (Fig. 1). Interestingly, the BY4741 strain exhibited a slight increase in fluconazole susceptibility compared to the

BY4741 *hap1Δ* strain (Fig. 1A and C). We suspect that the enhanced azole susceptibility in the BY4741 strain is because of a known insertion of an in-frame *Ty1* sequence at the 3' end of the *HAP1* ORF, resulting in the expression of a mutated *HAP1* that lacks 13 amino acids from its C-terminus and contains an additional 32 amino acids encoded from the *Ty1* sequence. The insertion of the *Ty1* element does not seem to affect the growth of BY4741 (*hap1-Ty1* mutant) versus FY2609 (*HAP1* WT) under untreated conditions (Fig. 1A-C, Table S1). In contrast, deletion of *HAP1* (FY2611 *hap1Δ*) showed a hypersusceptible phenotype compared to FY2609 when grown on agar plates or in liquid culture containing 32 µg/mL fluconazole (Fig. 1A and C). In addition, both the FY2611 *hap1Δ* strain and the BY4741 *hap1Δ* strain have a similar doubling time in the presence and absence of fluconazole (Fig. 1A-C and Table S1). To our knowledge, this is the first observation that Hap1 contributes to azole susceptibility in *S. cerevisiae*. We suspect that this phenotype has not been observed until now because earlier functional genomics screens used the BY4741 and BY4742 parental and deletion strain collections (47).

Phylogenetic analysis of Hap1 homologs in pathogenic fungi.

A phylogenetic tree was constructed to investigate the evolutionary relationships of *S. cerevisiae* Hap1 homologs in the human pathogen *C. glabrata* and other fungal species. Two genes, Zinc cluster factor 4 (Zcf4) and Zinc cluster factor 27 (Zcf27), in *C. glabrata* grouped within the Hap1 clade of transcription factors (Fig. 2 and S1). *C. glabrata* is now recognized as a member of the *Nakaseomyces* genus (48). In our phylogeny, Zinc cluster factor 4 (Zcf4) and Zinc cluster factor 27 (Zcf27) in *C. glabrata* group with two non-pathogenic species of *Nakaseomyces*, *N. delphensis*, and *N. bacillisporus*. Although *Cg*Zcf4 groups more closely with *Sc*Hap1 in the tree compared to *Cg*Zcf27, support for the association is weak (ultrafast bootstrap support < 90). In general, the branching pattern of the Hap1 gene tree does not match the expected species relationships as determined by whole genome phylogenomic analysis (49). This suggests a complicated evolution history for this gene family including gene/genome duplication, gene loss,

and possible horizontal gene transfer (50). The timing of the duplication event that gave rise to Zcf4 and Zcf27 in the *Nakaseomyces* clade is unclear. The duplication could have occurred in a common ancestor of *S. cerevisiae* and *C. glabrata,* and one copy was subsequently lost in *S. cerevisiae*. An alternative explanation is that the duplication occurred after the *Nakaseomyces*-*Saccharomyces* split.

Zcf27, rather than, Zcf4 alters azole susceptibility in *C. glabrata*.

Because deletion of *HAP1* in *S. cerevisiae* altered azole susceptibility, we wanted to determine if *C. glabrata* strains lacking their Hap1 homologs Zcf27 and Zcf4 have a similar susceptibility to azole drugs. To test this hypothesis, we deleted *ZCF4* and *ZCF27* in the *C. glabrata* CBS138 (ATCC *Cg*2001) WT strain and performed liquid growth and serial-dilution spot assays with and without 32 µg/mL fluconazole (Fig. 3A-C). In the untreated conditions, both *zcf27Δ* and *zcf4Δ* strains grew similar to the *Cg*2001 WT strain on agar plates and liquid cultures (Fig. 3A-C). We also did not observe any differences in doubling times (Table S2). However, in the presence of fluconazole, the *zcf27Δ* strain showed an azole hypersusceptibility phenotype on agar plates along with a growth delay and longer doubling times when cultured in liquid media, whereas *zcf4Δ* strain grew like the *Cg*2001 WT strain (Fig. 3A and C, Table S2). To confirm that our observed azole hypersusceptible phenotype was due to the loss of *ZCF27*, the full-length *ZCF27* open-reading frame with its endogenous promoter were cloned in the pGRB2.0 plasmid and transformed into a *Cg*989 *zcf27Δ* deletion strain (Table S3 and S4). The pGRB2.0 vector was also transformed into *Cg*989 (ATCC 200989) as a control (Table S3 and S4). The *ZCF27* plasmid construct was able to rescue azole susceptibly as shown by a serial-dilution spot assay (Fig. 3D) while the *zcf27Δ* strain expressing the plasmid only construct remain hypersusceptible (Fig. 3D). In addition, gene expression analysis also confirmed that *ZCF27* and *ZCF4* were not expressed in their respective deletion strains (Fig. S2A and B). In addition, we confirmed that the genes upstream and downstream of *ZCF27* were expressed in *zcf27Δ* similar to the *Cg*2001

183 WT strain (Fig. S3A and B). Finally, we also deleted the upstream (*CAGL0K05819g*) and
184 downstream (*CAGL0K05863g*) genes and observed no change in azole susceptibility (Fig.
185 S3C). Overall, our data shows that Zcf27, rather than Zcf4, plays a specific role in mediating
186 azole susceptibility.
187
188 **Expression of *CYC1* depends on Zcf27, but not Zcf4 because of differences in protein**
189 **expression.**
190 In *S. cerevisiae* Hap1 is known to regulate the expression of the *CYC1* gene (51-55). To
191 determine if Zcf27 and/or Zcf4 also controls the expression of *C. glabrata CYC1* gene, *Cg*2001
192 WT, *zcf27Δ*, and *zcf4Δ* strains were grown in the presence and absence of azole treatment and
193 qRT-PCR transcript analysis was performed. Interestingly, *CYC1* transcript analysis revealed
194 that the loss of *ZCF27*, but not *ZCF4*, resulted in a 50% decrease in *CYC1* expression,
195 irrespective of drug treatment (Fig. 4A and B). To determine if this difference was a
196 consequence of transcript levels of *ZCF4* and *ZCF27,* qRT-PCR analysis was performed on
197 *Cg*2001 WT cells treated with or without 64 µg/mL fluconazole for 3 or 6 hours. Both *ZCF27* and
198 *ZCF4* transcript levels were expressed with no significant differences between untreated and
199 fluconazole treated conditions (Fig. 4C and D; Table S7). Furthermore, *ZCF27* transcript levels
200 are not altered in *zcf4Δ* strain and vice versa indicating they are independent of each other (Fig.
201 S2A and B). To determine if protein expression levels differed between Zcf27 and Zcf4, we
202 constructed endogenously 3XFLAG tagged strains where the 3XFLAG tag was inserted at the
203 C-terminus of *ZCF27* and *ZCF4*. After PCR confirmation, Zcf27-3XFLAG and Zcf4-3XFLAG
204 tagged strains were grown with or without 64 µg/mL fluconazole for 3 or 6 hrs. Western blot
205 analysis indicated that the Zcf27-3XFLAG protein expression remained fairly constant with and
206 without drug treatment (Fig. 4E). Unexpectedly, we observed virtually no expression of Zcf4-
207 3XFLAG protein regardless of drug treatment (Fig. 4E, Short Exp). Even with longer exposure
208 times, barely detectable levels of Zcf4 were observed (Fig. 4E, Long Exp) suggesting that Zcf4

is regulated at the post-transcriptional level. Due to essentially undetectable levels of Zcf4 protein, we suspect that this is why a *zcf4Δ* strain does not alter *CYC1* gene expression or show hypersusceptibility to azoles.

Zcf27 is dispensable for expression of drug efflux pumps but is needed for azole-induced expression of ergosterol (*ERG*) genes.

Because the *zcf27Δ* strain showed altered azole susceptibility (Fig.3A-C), we wanted to identify the mechanism mediating this phenotype. A common mechanism of altering azole resistance in *C. glabrata* involves the upregulation of drug efflux pumps such as *CDR1*, *PDH1*, and *SNQ2*, facilitated by the zinc cluster transcription factor Pdr1 (28, 29, 31, 56, 57). To determine if expression of drug efflux pumps is altered in the *zcf27Δ* strain in the presence or absence of 64 µg/mL fluconazole, the expression levels of the known azole transporters *CDR1, PDH1,* and *SNQ2* as well as the transcriptional regulator *PDR1* were analyzed by qRT-PCR analysis. Our transcript analysis revealed no significant difference in the expression of any of the genes encoding ABC-transporters in the *zcf27Δ* strain compared to the *Cg*2001 WT strain (Fig. 5A and B; S4A and B) indicating that altered expression of azole drug efflux pumps is not the reason for azole hypersusceptibility for the *zcf27Δ* strain.

In *S. cerevisiae*, Hap1 is known to regulate steady state transcript levels of ergosterol biosynthesis genes such as *ERG11*, *ERG3*, *ERG5* and *ERG2* (40, 41, 44, 52, 53, 58, 59) . In addition, altered *ERG11* gene expression in *C. glabrata* is also a mechanism that can lead to azole hypersusceptibility phenotypes (24, 60, 61). To determine if altered *ERG* gene expression was a mechanism for the observed azole hypersusceptibility of the *zcf27Δ* strain, *Cg*2001 WT and *zcf27Δ* strains were treated with and without 64 µg/mL fluconazole and *ERG11*, *ERG3*, *ERG5* and *ERG2* transcript levels were analyzed by qRT-PCR. In the absence of drug, with the exception of *ERG3*, no significant difference in the expression levels of *ERG11*, *ERG5* or *ERG2* was observed between the *Cg*2001 WT and *zcf27Δ* strain (Fig. 5C-F). However, upon treatment

with fluconazole, all four *ERG* genes failed to induce to wild-type levels in the *zcf27Δ* strain (Fig. 5C-F). Furthermore, a *zcf4Δ* strain did not have altered *ERG11* and *ERG3* expression which coincides with its lack of expression and azole hypersusceptible phenotype (Fig. S4C and D). Altogether, our data indicates that in addition to Upc2A, Zcf27 serves as another critical transcription factor for the azole-induced expression of the late ergosterol pathway genes.

Zcf27-3XFLAG is enriched at *ERG* gene promoters.

Because our data shows decreased expression of ergosterol genes in the *zcf27Δ* strain upon azole treatment (Fig. 5C-F), we suspect that Zcf27 is a direct transcription factor for the *ERG* genes. To determine if Zcf27 directly targets the promoter of the *ERG11* gene, chromatin immunoprecipitation (ChIP) assays were performed using anti-FLAG monoclonal antibodies and chromatin isolated from untagged *Cg*2001 WT and Zcf27-3XFLAG strains, treated with or without fluconazole. ChIP-qPCR fluorescent probes were designed to recognize a distal (E11P1) and proximal (E11P2) promoter region of *ERG11*. Using these probes, a significant enrichment of Zcf27 was detected at both *ERG11* promoter regions compared to the untagged control (Fig. 6A and B; Table S8). In addition, Zcf27 was further enriched at the promoter of *ERG11* upon azole treatment (Fig. 6A and B; Table S8) supporting the importance of Zcf27 in azole-induced gene expression. No significant enrichment of Zcf27 was detected at the 3'*UTR* of *ERG11* regardless of treatment (Fig. S5), indicating specific enrichment at the promoter region.

We also examined Zcf27 localization status on the *ERG3* promoter by ChIP analysis (Fig 6C and D). To determine if Zcf27 binds to the promoter of *ERG3,* two ChIP-qPCR fluorescent probes were designed to recognize the distal (E3P1) and proximal (E3P2) promoter regions. Similar to the *ERG11* promoter, Zcf27 was detected at the distal *ERG3* promoter region and was further enriched upon fluconazole treatment (Fig. 6C and Table S8). However, we did not detect any Zcf27 enrichment at the more proximal promoter region (Fig. 6D and Table S8) regardless

of azole treatment. Overall, our data demonstrates that Zcf27 directly targets the promoters of *ERG11* and *ERG3* to help facilitate the proper expression of *ERG* genes and maintenance of ergosterol homeostasis during azole treatment.

The *zcf27Δ* strain has altered azole susceptibility due to decreased ergosterol levels, which can be suppressed by exogenous sterols and active sterol import.

Because azole-induced *ERG* gene expression is diminished in the *zcf27Δ* strain, we would expect an additional decrease in ergosterol levels in this strain, which would explain why a *zcf27Δ* strain has an increase in azole susceptibility. To ascertain whether total endogenous ergosterol levels differed between *Cg*2001 WT and *zcf27Δ* strains upon azole treatment, non-polar lipids were extracted from both strains in the presence and absence of 64 µg/mL fluconazole. Total ergosterol level was measured by high performance liquid chromatography (HPLC) analysis and cholesterol was used as an internal standard control. No significant difference was observed between *Cg*2001 WT and *zcf27Δ* strains in the untreated conditions, concurring with our gene expression analysis showing no significant difference in expression of multiple *ERG* genes without azole treatment (Fig. 7A). However, upon fluconazole treatment, the *Cg*2001 WT strain demonstrated the expected decrease in ergosterol levels (Fig. 7B), whereas the *zcf27Δ* strain exhibited an additional 30% reduction in total ergosterol compared to the treated *Cg*2001 WT strain (Fig. 7C).

Due to this observation, we hypothesized that the decrease in ergosterol content contributes to azole hypersensitivity and reasoned that exogenous supplementation with ergosterol would suppress the azole hypersensitive phenotype observed for the *zcf27Δ* strain. To test this hypothesis, *Cg*2001 WT and *zcf27Δ* strains were plated on synthetic complete (SC) media supplemented with or without exogenous ergosterol and/or fluconazole. In support of our hypothesis, serial-dilution spot assays showed that the addition of exogenous ergosterol completely suppressed the azole hypersensitive phenotype of the *zcf27Δ* strain, whereas

zcf27Δ strain without ergosterol retained the hypersensitive phenotype (Fig. 7D). Because ergosterol is solubilized in the presence of Tween 80-ethanol solution, we wanted to determine if this suppression was specific to ergosterol. Thus, *Cg*2001 WT and *zcf27Δ* strains were plated on SC media supplemented with a Tween 80-ethanol solution with or without fluconazole. As indicated in supplemental Fig. S6, Tween 80-ethanol did not suppress *zcf27Δ* azole hypersusceptible phenotype (Fig. S6) indicating that suppression was mediated by exogenous ergosterol uptake.

Based on these observations, we also expected that deletion of the only known sterol importer *AUS1* would prevent sterol uptake by *zcf27Δ* strains (62-64). To determine this, we constructed an *aus1Δ* strain and a *zcf27Δaus1Δ* double deletion strain and performed serial-dilution spot assays on agar plates supplemented with or without exogenous ergosterol in the presence and/or absence of fluconazole (Fig. 7E). As anticipated, the *zcf27Δaus1Δ* strain remained hypersensitive to fluconazole with or without exogenous ergosterol (Fig. 7E). However, growth of the *aus1Δ* strain was not altered by fluconazole and/or exogenous ergosterol and grew similar to the *Cg*2001 WT strain (Fig. 7E). Overall, our data elucidates the mechanistic basis and pathway underlying the hypersensitive phenotype observed in the *zcf27Δ* strain. Because Zcf4 is not expressed, it is unclear what role it plays, if any, under azole treatment. In summary, our findings represent the first characterization of Zcf27 as direct transcription factor for regulating ergosterol genes and ergosterol homeostasis in response to azole drug treatment.

Zcf4 is induced upon hypoxic exposure.

In aerobic conditions, *S. cerevisiae* Hap1 functions as a transcriptional activator of *CYC1* and *ERG* genes (40, 41, 44, 51-55, 58, 59). Furthermore, our presented data suggests that Zcf27 operates similarly to Hap1, by regulating the corresponding conserved genes in *C. glabrata*. Interestingly, in *S. cerevisiae*, Hap1 functions also as a transcriptional repressor to shut down

313 *ERG* genes under hypoxia by recruiting a corepressor complex containing Set4, Tup1, and
314 Ssn6 corepressors (40, 59, 65, 66). Currently, it is not known if Zcf27, Zcf4 or another
315 transcription factor functions to repress *C. glabrata ERG* genes under hypoxic conditions.
316 Due to our observed phenotype for the *zcf27Δ* strain, but not for the *zcf4Δ* strain under
317 azole treated conditions, *C. glabrata Cg*2001 WT, *zcf27Δ*, and *zcf4Δ* strains were serially diluted
318 five-fold on agar plates and grown under aerobic or hypoxic conditions (Fig. 8A). Interestingly,
319 under hypoxic conditions, only the *zcf4Δ* strain exhibited a statistically significant slow growth
320 defect, as determined by colony size (Fig. 8A and B). Measuring the colony diameter revealed
321 an approximate 40% decrease in the size of *zcf4Δ* colonies when compared to both the *Cg*2001
322 WT and the *zcf27Δ* colonies suggesting a potential function for Zcf4 (Fig. 8B). Due to the
323 significant differences in protein expression observed between Zcf27 and Zcf4 under aerobic
324 conditions, we also evaluated the transcript and protein expression levels of Zcf4 and Zcf27
325 under hypoxic conditions. Using qRT-PCR analysis, a 4-fold increase in *ZCF4* transcript levels
326 was detected after two hours under hypoxic conditions while *ZCF27* transcript levels remained
327 unaltered from aerobic to hypoxic conditions (Fig. 8C and D). In addition, we assessed the
328 protein levels of Zcf4-3XFLAG and Zcf27-3XFLAG tagged strains using Western blot analysis.
329 Remarkably, we detected robust levels of Zcf4 proteins under hypoxic conditions while Zcf27
330 protein levels remained the same from aerobic to hypoxic conditions (Fig. 8E and F). Taken
331 together, we have identified Zcf4 as the first hypoxia-inducible transcription factor in *C. glabrata*.
332 Given that *S. cerevisiae* Hap1 is required for repressing *ERG* genes under hypoxic conditions,
333 we anticipate that Zcf4 is hypoxia-induced to function in a similar manner.
334
335 **Ergosterol genes are downregulated upon hypoxic conditions**
336 In *S. cerevisiae,* it is well established that exposure to hypoxia leads to the repression of the
337 *ERG* pathway (40, 59, 65). To determine if hypoxia-mediated repression of *ERG* genes is
338 conserved and robust in *C. glabrata*, as observed in *S. cerevisiae*, we performed transcript

analysis of multiple *ERG* genes involved in the late ergosterol biosynthesis pathway, namely, *ERG11*, *ERG3, ERG2*, *ERG5*. When comparing the indicated *ERG* gene transcript levels under aerobic versus hypoxic conditions, we observed a significant decrease of 70-90% in expression under hypoxic conditions (Fig. 9A-D). These findings confirm that a conserved mechanism between *S. cerevisiae* and *C. glabrata* is maintained for shutting down ergosterol biosynthesis in response to hypoxic conditions.

Zcf4, rather than Zcf27, represses genes from ergosterol pathway under hypoxic conditions.

In *S. cerevisiae,* it is known that following exposure to hypoxia *ERG* genes are repressed by a WT copy of *HAP1* but not by *hap1-Ty1* expressed in S288C strains (40, 59, 65). To determine if Zcf27 and/or Zcf4 shares the same function as Hap1 under hypoxic conditions, qRT-PCR analysis on *ERG* genes were performed. Surprisingly, our transcript analysis did not detect any significant differences in the transcript levels of *ERG11*, *ERG3*, *ERG5* and *ERG2* between the *Cg*2001 WT and *zcf27Δ* strain under hypoxic conditions (Fig. 10A-D). In contrast, we observed a significant increase in the transcript levels of *ERG11*, *ERG3*, and *ERG5* genes in the *zcf4Δ* compared to *Cg*2001 WT strain (Fig. 10 E-G). Interestingly, *ERG2* showed no significant difference in the transcript levels upon hypoxic exposure in either *zcf27Δ* or *zcf4Δ* strain (Fig. 10D and H), despite being repressed upon hypoxic exposure (Fig. 9C) indicating involvement of another transcription factor. Overall, our findings suggest that Zcf4, rather than Zcf27, is directly or indirectly involved in hypoxia-induced *ERG* gene repression.

Both Zcf4-3XFLAG and Zcf27-3XFLAG are enriched on *ERG11* and *ERG3* gene promoter upon hypoxic exposure.

Because we determined that Zcf27 was enriched at the promoter sequences of *ERG11* and *ERG3* under aerobic azole conditions, we wanted to assess the direct binding of Zcf27 and Zcf4

at *ERG* gene promoters under hypoxic conditions. To determine this, ChIP assays were performed using anti-FLAG monoclonal antibodies and chromatin isolated from untagged *Cg*2001 WT, Zcf27-3XFLAG and Zcf4-3XFLAG strains grown for 8 hours under hypoxic conditions. The same ChIP-qPCR fluorescent probes used under azole-treated conditions were utilized to assess the enrichment of Zcf27 and Zcf4 at the *ERG11* and *ERG3* promoters. At the *ERG11* promoter, Zcf27 showed 3.5-fold enrichment at the proximal promoter sequence but was not enriched at the more distal promoter sequence (Fig. 11A and B). Interestingly, this differs from our observations under azole treated conditions, where Zcf27 was more enriched at the distal promoter sequence than the more proximal promoter sequence (Fig. 6A and B). For Zcf4, we observed a 5-fold enrichment at the *ERG11* distal promoter sequence compared to untagged *Cg*2001 WT strain, but no enrichment was observed at the proximal promoter sequence (Fig. 11C and D). In addition, Zcf27 and Zcf4 enrichment was specific to the promoter of *ERG11* since no significant enrichment was observed at the 3'*UTR* of *ERG11* (Fig. S7A and B). At the *ERG3* promoter, Zcf27 showed a 3-fold enrichment at the proximal promoter sequence but was not enriched at the distal promoter sequence (Fig. 11E and F). Again, this differs from our observations under azole treated conditions where Zcf27 enriches exclusively at the *ERG3* distal promoter sequence but not at the proximal promoter sequence (Fig 6C and D). In contrast, under hypoxic conditions, Zcf4 was 2-fold enriched at the *ERG3* distal promoter sequence but 20-fold enriched at the proximal promoter sequence suggesting the Zcf4 occupies both sites but prefers the more proximal sequence (Fig. 11G and H). Based on our observations, Zcf4 binding at these promoters likely prevents efficient binding of Zcf27 and Upc2A under hypoxic conditions so that *ERG* gene repression can occur.

DISCUSSION

In this study, the roles of the *S. cerevisiae* Hap1 zinc cluster transcription factor homologs, Zcf27 and Zcf4, were investigated in response to azole drug treatment and hypoxic conditions.

Our data suggest that Zcf27 functions similarly to *Sc*Hap1 under aerobic conditions, regulating the conserved genes *CYC1* and *ERG3* under untreated conditions. Additionally, we found that loss of *ZCF27*, but not *ZCF4*, impacts azole susceptibility due to the inability to adequately induce *ERG* genes under azole drug treatment and maintain ergosterol homeostasis. Furthermore, we discovered that Zcf4 is specifically expressed in response to hypoxia, allowing it to function as a repressor of *ERG* genes. Overall, our study revealed that *C. glabrata* maintains two Hap1 homologs, Zcf27 and Zcf4, to control gene expression and mediate proper ergosterol homeostasis in response to both azole drug treatment and hypoxic conditions (see model Fig. 12A and B).

Our phylogenetic analysis positions Zcf27 and Zcf4 as the closest homologs to *S. cerevisiae* Hap1 where we have determined that Zcf27 alters azole susceptibility, unlike Zcf4. Although Upc2A is the major transcription factor associated with azole-mediated induction of *ERG* genes, our study provides new insights into an additional transcriptional regulator besides Upc2 that is needed for azole-induced expression of *ERG* genes. Additional genetic and biochemical studies will be needed to determine the mechanism by which Zcf27 and Upc2A operate together in response to azole drugs. Nonetheless, we speculate that Zcf27 could mediate either a direct or indirect cooperative event that assists Upc2A in fully inducing ergosterol genes (see model Fig 12A and B). Additionally, in *S. cerevisiae*, deleting both Upc2 and its paralog Ecm22 further alters azole drug susceptibility, resistance to amphotericin B, and *ERG* gene expression (42, 43, 45, 65). Thus, Upc2A and Zcf27 may be operating in an analogous manner. However, there exists a distinct possibility that other yet-to-be identified zinc cluster transcription factors could be involved in regulating *ERG* gene expression. Identifying additional transcription factors besides Zcf27 and Upc2A will be important to fully understand what contributes to azole susceptibility and/or clinical drug resistance.

In contrast to Zcf27, Zcf4 protein levels were nearly undetectable under aerobic and/or azole treated conditions, with significant induction observed only under hypoxic conditions. This

417 explains why the *ZCF4* deletion strain lacks an azole hypersensitive phenotype or any alteration
418 in *ERG* gene expression. Based on our data, Zcf4 protein levels are likely being regulated by an
419 unknown post-transcriptional mechanism. Although we have not identified the regulatory
420 mechanism governing Zcf4 protein levels, we suspect that it is degraded via a specific ubiquitin
421 ligase. Zcf4 may also be regulated in a manner similar to human HIF-1α (67, 68). To our
422 knowledge, Zcf4 represents the first identified hypoxia-induced zinc cluster transcription factor
423 and understanding the precise mechanism of protein degradation would be of interest.
424 Although deletion of Zcf4, also called Mar1 (Multiple Azole Resistance 1), has been
425 initially described to alter azole susceptibility when treated with high concentrations of azoles,
426 we have not been able to confirm this with our studies (34, 39). Currently, it is unclear the
427 reason behind these discrepancies, but there could be differences in *C. glabrata* strains or
428 conditions where Zcf4 is expressed at higher levels than what we have observed. However, the
429 findings by Gale et al., utilizing a *C. glabrata* BG14 strain and employing a *Hermes* transposon
430 approach to screen for fluconazole susceptibility, provided support for our observations (69). In
431 their study, they identified several genes that when disrupted, altered azole drug susceptibility,
432 including Zcf27 but not Zcf4 (69). More studies will be needed to completely understand the role
433 of Zcf4 in azole susceptibility, if any, and how it is regulated at the transcriptional and post-
434 transcriptional level. Nonetheless, our results are clear and consistent where Zcf4 plays a
435 hypoxia-specific role in repressing *ERG* genes. We suspect that Zcf4, similar to Hap1 in *S.*
436 *cerevisiae*, operates with a corepressor complex to repress *ERG* genes (59, 65, 66). Hypoxia-
437 induced expression of Zcf4 and the growth defect observed in the *zcf4Δ* strain under hypoxic
438 conditions highlight its importance in metabolic adaptation and survival in oxygen-limited
439 environments. In addition, it is likely Zcf4 hypoxia-specific induction plays additional roles for *C.*
440 *glabrata* to survive and propagate under low oxygen while within the humans.
441 Overall, this study expands our understanding of the transcriptional regulation of
442 ergosterol biosynthesis in *C. glabrata*. This is significant because targeting ergosterol and/or

443 enzymes involved in ergosterol biosynthesis have yielded highly useful and effective antifungals
444 (66, 70, 71). Thus, studies focused on the regulatory mechanisms of this pathway could lead to
445 the development of targeted antifungal therapies and help in overcoming the challenge of azole
446 resistance in clinical settings. Because zinc cluster transcription factors are unique to fungi and
447 not found in humans (32), there could be an opportunity to explore them as drug targets.
448 Overall, our findings reveal a novel regulatory mechanism where Zcf27 and Zcf4 are
449 differentially employed by *C. glabrata* to manage ergosterol biosynthesis and maintain
450 membrane integrity under varying environmental conditions. Our findings provide some of the
451 first insights into functional role of two zinc cluster transcription factors. We suspect that further
452 studies on these and similar factors will enhance our understanding of the pathophysiology and
453 drug resistance mechanisms of *C. glabrata*.
454

455 **MATERIALS AND METHODS**

456 **Plasmids and yeast strains**

457 All plasmids and yeast strains are described in Table S3 and Table S4. The S288C BY4741
458 *S. cerevisiae* strain was obtained from Open Biosystems. The S288C strain containing the
459 *HAP1-Ty1* sequence was corrected with a wild-type copy of *HAP1* (FY2609) and the *HAP1*
460 deletion strain (FY2611) was kindly provided to us by Dr. Fred Winston, Department of
461 Genetics, Harvard Medical School (40). *C. glabrata* 2001 (CBS138, ATCC 2001) and *C.*
462 *glabrata* ATCC 200989 were acquired from the American Type Culture Collection (72). For Zcf27
463 complementation assays, a genomic fragment containing the *ZCF27* promoter, *5' UTR*, open
464 reading frame (ORF), and *3' UTR* was PCR-amplified and cloned into the pGRB2.0 plasmid
465 (Addgene) (73) using restriction enzymes BamHI and SacII. For endogenous C-terminal epitope
466 tagging, a 3XFLAG-NatMX cassette was PCR-amplified from pYC46 plasmid (Addgene) and
467 inserted at the C-terminus of *ZCF27* and *ZCF4* (74, 75). All *C. glabrata* strains were created
468 using the CRISPR-Cas9 RNP system as previously described (74). Briefly, for generating

deletion strains, two CRISPR gRNAs were designed near the 5′ and 3′ ORFs of the gene of interest. Drug-resistant selection markers were PCR-amplified using Ultramer DNA Oligos (IDT) from pAG32-HPHMX6 (hygromycin) or pAG25-NATMX6 (nourseothricin). For 3XFLAG epitope tagging, one CRISPR gRNA was designed in the *3′ UTR* of the gene of interest. Cells were then electroporated with the CRISPR-RNP mix and the drug resistance cassette.

Serial-dilution spot and liquid growth assay.

For serial-dilution spot assays, yeast strains were grown to saturation overnight in SC at 30°C. Cells were diluted to OD_{600} of 0.1 and allowed to grow to exponential phase with continuous shaking at 30°C. Each strain was then spotted in five-fold dilution starting at an $O.D_{600}$ of 0.01 on untreated SC agar plates or plates containing 32 µg/ml fluconazole (Cayman). Plates were grown at 30°C for 2 days. For liquid growth assay, the yeast strains were inoculated in SC media and grown to saturation overnight. The cultures were then diluted to an OD_{600} of 0.1 and grown to log phase with shaking at 30°C. Upon reaching log phase, the strains were diluted to an OD_{600} of 0.001 in a 96 well round bottom plate containing 100 µL of SC media with and without 32 µg/ml fluconazole (Cayman). Cells were grown in liquid culture for 50 hours with shaking at 30°C, and the OD_{600} was measured every 15 minutes using a Bio-Tek Synergy 4 multimode plate reader. For spot assays under hypoxia, YPD plates were placed inside the BD Gaspak EZ anaerobe gas generating pouch system with indicator (BD 260683) after spotting and incubated for up to 7 days. Hypoxic cell collection for qRT-PCR, Western blot, and ChIP assays was performed by growing the indicated yeast strains in YPD media for 8 hours using the BD GasPak EZ anaerobe gas generating pouch system (BD 260683). Cells were immediately spun down for one minute and flash frozen to maintain the hypoxic state.

Phylogenetic analysis

494 For the phylogenetic tree construction, 90 gene sequences were curated based on high-scoring
495 BLAST hits to *Sc*Hap1. Of these sequences, 83 were retrieved from Mycocosm and 7 from the
496 *Candida* Genome Database (76, 77), including CAGL0B03421g (*Cg*Zcf4), CAGL0K05841g
497 (*Cg*Zcf27), B9J08_004061, B9J08_002924, B9J08_002930, B9J08_004353, and
498 B9J08_002931. Protein sequence alignments were performed by Multiple Alignment using
499 MAFFT version 7.471 (options: --auto) using the E-INSI iterative refinement method (78). The
500 aligned sequences were then used to generate a maximum-likelihood phylogenetic tree with IQ-
501 TREE version 1.5.5, using the built-in ModelFinder to determine the best-fit nucleic acid
502 substitution model and 1000 ultrafast bootstrap replicates (79). The tree was visualized using
503 Figtree software version 1.4.4 (http://tree.bio.ed.ac.uk/software/figtree/).
504
505 **Quantitative real-time PCR analysis**
506 RNA was isolated from strains grown in SC or YPD using standard acid phenol purification
507 method. 1 µg RNA was reverse-transcribed to cDNA using the All-in-One 5x RT Mastermix kit
508 (ABM). Gene expression primers were designed using Primer Express 3.0 software and are
509 listed in Table S5. Quantitative real-time polymerase chain reaction (qRT-PCR) values are
510 indicated in Table S7 and S9. At least 3 biological replicates, including three technical replicates,
511 were performed for all samples. Data were analyzed by the comparative C_T method ($2^{-\Delta\Delta CT}$)
512 where *RDN18* (18S rRNA) was used as an internal control. All samples were normalized to
513 untreated untagged wild-type strain. GraphPad Prism version 9.5.1 was used to determine the
514 unpaired t-test for determining statistical significance.
515
516 **Yeast extraction and Western blot analysis**
517 The indicated yeast strains were grown in SC or YPD media under aerobic or hypoxic condition.
518 Yeast whole cell extraction and Western blot analysis to detect Zcf4-3XFLAG, Zcf27-3XFLAG
519 and Histone H3 were performed as previously described (78). The monoclonal FLAG M2 mouse

antibody (F1804, Sigma-Aldrich) was used at a 1:5000 dilution to detect Zcf4-3XFLAG and Zcf27-3XFLAG at 1:5000 dilution as previously described (59). The histone H3 rabbit polyclonal antibody (PRF&L) was used at a 1: 100,000 dilution as previously described (74).

Chromatin Immunoprecipitation

Chromatin immunoprecipitation was performed using ZipChIP as previously described (79). Briefly, 50 mL cultures of indicated yeast strains were grown to exponential phase (OD_{600} of 0.6) in SC or YPD media with or without shaking at 30°C under aerobic or 8h of hypoxic condition, respectively. Cells grown in SC media under aerobic condition were treated with 64 µg/mL fluconazole (Cayman) for 3 h and collected. Cells were then formaldehyde cross-linked for 15 min and harvested as previously described (79). The cells were lysed by bead-beating with glass beads and lysate was separated from beads. Upon separation, cell lysates were transferred to Diagenode Bioruptor Pico microtubes and sonicated with a Diagenode Bioruptor Pico at the high frequency setting for 30 s ON and 30 s OFF for 20 cycles. After sonication, cell lysates were pre-cleared with 5 µl of unbound protein G magnetic beads (10004D, Invitrogen) for 30 min with rotation at 4°C. 300 µl of precleared lysate was immunoprecipitated with 10 µl of protein G- magnetic beads (10004D, Invitrogen) conjugated to 1 µl of M2 FLAG antibody (F1804, Sigma-Aldrich). Probe and primer sets used for qPCR analysis are described in Table S6, and qPCR values are indicated in Table S8 and S10

Ergosterol extraction

Ergosterol was extracted from indicated strains as previously described (60, 80). Cultures were grown overnight in SC minimal media. Saturated cultures were back diluted to OD_{600} of 0.1 and were grown at 30°C to exponential phase (OD_{600} of 0.6), with or without 64 µg/ml fluconazole treatment. Sterols were extracted from yeast using 4 M potassium hydroxide in 70% (vol/vol) ethanol at 85°C for 1 h. After extraction, nonpolar lipids were separated by washing with

546 methanol twice. Nonpolar sterols were crystallized after evaporating the n-hexane and dissolved
547 in 100% methanol. Samples were analyzed by HPLC using a C18 column with a flow rate of 1
548 mL/min of 100% methanol. Ergosterol was detected at 280 nm, and cholesterol, used as an
549 internal control for extraction, was detected at 210 nm.
550

551 **ACKNOWLEGEMENTS**

552 This publication was supported by grants from the NIH National Institute of Allergy and
553 Infectious Diseases to S.D.B. (AI136995) and to J.B.G (T32AI148103). Funding support was
554 also provided from Purdue University AgSEED program (to S.D.B), Purdue Institute for Cancer
555 Research (Grant P30CA023168: Bindley Metabolite Profiling Facility), Department of
556 Biochemistry Bird Stair Fellowship (to D.S.), and NIFA 1007570 (to S.D.B).
557
558
559 **REFERENCE**

560 1. Denning DW. 2024. Renaming Candida glabrata-A case of taxonomic purity over clinical
561 and public health pragmatism. PLoS Pathog 20:e1012055.
562 2. Fang W, Wu J, Cheng M, Zhu X, Du M, Chen C, Liao W, Zhi K, Pan W. 2023. Diagnosis
563 of invasive fungal infections: challenges and recent developments. Journal of Biomedical
564 Science 30:42.
565 3. Delaloye J, Calandra T. 2014. Invasive candidiasis as a cause of sepsis in the critically ill
566 patient. Virulence 5:161-169.
567 4. Brunke S, Hube B. 2013. Two unlike cousins: Candida albicans and C. glabrata infection
568 strategies. Cell Microbiol 15:701-8.
569 5. Husni R, Bou Zerdan M, Samaha N, Helou M, Mahfouz Y, Saniour R, Hourani S, Kolanjian
570 H, Afif C, Azar E, El Jisr T, Mokhbat J, Abboud E, Feghali R, Abboud E, Matta H,
571 Karayakouboglo G, Matar M, Moghnieh R, Daoud Z. 2023. Characterization and
572 susceptibility of non-albicans Candida isolated from various clinical specimens in
573 Lebanese hospitals. Front Public Health 11:1115055.
574 6. Turner SA, Butler G. 2014. The Candida pathogenic species complex. Cold Spring Harb
575 Perspect Med 4:a019778.
576 7. Dujon B, Sherman D, Fischer G, Durrens P, Casaregola S, Lafontaine I, De Montigny J,
577 Marck C, Neuvéglise C, Talla E, Goffard N, Frangeul L, Aigle M, Anthouard V, Babour A,
578 Barbe V, Barnay S, Blanchin S, Beckerich JM, Beyne E, Bleykasten C, Boisramé A, Boyer
579 J, Cattolico L, Confanioleri F, De Daruvar A, Despons L, Fabre E, Fairhead C, Ferry-
580 Dumazet H, Groppi A, Hantraye F, Hennequin C, Jauniaux N, Joyet P, Kachouri R, Kerrest
581 A, Koszul R, Lemaire M, Lesur I, Ma L, Muller H, Nicaud JM, Nikolski M, Oztas S, Ozier-
582 Kalogeropoulos O, Pellenz S, Potier S, Richard GF, Straub ML, et al. 2004. Genome
583 evolution in yeasts. Nature 430:35-44.

8. Crunden JL, Diezmann S. 2021. Hsp90 interaction networks in fungi—tools and techniques. FEMS Yeast Research 21.
9. Flevari A, Theodorakopoulou M, Velegraki A, Armaganidis A, Dimopoulos G. 2013. Treatment of invasive candidiasis in the elderly: a review. Clin Interv Aging 8:1199-208.
10. Pappas PG, Lionakis MS, Arendrup MC, Ostrosky-Zeichner L, Kullberg BJ. 2018. Invasive candidiasis. Nature Reviews Disease Primers 4:18026.
11. Fidel PL, Jr., Vazquez JA, Sobel JD. 1999. Candida glabrata: review of epidemiology, pathogenesis, and clinical disease with comparison to C. albicans. Clin Microbiol Rev 12:80-96.
12. Kurtzman CP. 2003. Phylogenetic circumscription of Saccharomyces, Kluyveromyces and other members of the Saccharomycetaceae, and the proposal of the new genera Lachancea, Nakaseomyces, Naumovia, Vanderwaltozyma and Zygotorulaspora. FEMS Yeast Research 4:233-245.
13. Gabaldón T, Martin T, Marcet-Houben M, Durrens P, Bolotin-Fukuhara M, Lespinet O, Arnaise S, Boisnard S, Aguileta G, Atanasova R, Bouchier C, Couloux A, Creno S, Almeida Cruz J, Devillers H, Enache-Angoulvant A, Guitard J, Jaouen L, Ma L, Marck C, Neuvéglise C, Pelletier E, Pinard A, Poulain J, Recoquillay J, Westhof E, Wincker P, Dujon B, Hennequin C, Fairhead C. 2013. Comparative genomics of emerging pathogens in the Candida glabrata clade. BMC Genomics 14:623.
14. Whaley SG, Berkow EL, Rybak JM, Nishimoto AT, Barker KS, Rogers PD. 2016. Azole Antifungal Resistance in Candida albicans and Emerging Non-albicans Candida Species. Front Microbiol 7:2173.
15. Lass-Flörl C. 2011. Triazole Antifungal Agents in Invasive Fungal Infections. Drugs 71:2405-2419.
16. Kelly SL, Lamb DC, Corran AJ, Baldwin BC, Kelly DE. 1995. Mode of action and resistance to azole antifungals associated with the formation of 14 alpha-methylergosta-8,24(28)-dien-3 beta,6 alpha-diol. Biochem Biophys Res Commun 207:910-5.
17. Warrilow AG, Martel CM, Parker JE, Melo N, Lamb DC, Nes WD, Kelly DE, Kelly SL. 2010. Azole binding properties of Candida albicans sterol 14-alpha demethylase (CaCYP51). Antimicrob Agents Chemother 54:4235-45.
18. Sanglard D, Ischer F, Koymans L, Bille J. 1998. Amino acid substitutions in the cytochrome P-450 lanosterol 14alpha-demethylase (CYP51A1) from azole-resistant Candida albicans clinical isolates contribute to resistance to azole antifungal agents. Antimicrob Agents Chemother 42:241-53.
19. White TC. 1997. The presence of an R467K amino acid substitution and loss of allelic variation correlate with an azole-resistant lanosterol 14alpha demethylase in Candida albicans. Antimicrob Agents Chemother 41:1488-94.
20. Kelly SL, Lamb DC, Kelly DE, Manning NJ, Loeffler J, Hebart H, Schumacher U, Einsele H. 1997. Resistance to fluconazole and cross-resistance to amphotericin B in Candida albicans from AIDS patients caused by defective sterol delta5,6-desaturation. FEBS Lett 400:80-2.
21. Watson PF, Rose ME, Ellis SW, England H, Kelly SL. 1989. Defective sterol C5-6 desaturation and azole resistance: a new hypothesis for the mode of action of azole antifungals. Biochem Biophys Res Commun 164:1170-5.
22. Flowers SA, Barker KS, Berkow EL, Toner G, Chadwick SG, Gygax SE, Morschhäuser J, Rogers PD. 2012. Gain-of-function mutations in UPC2 are a frequent cause of ERG11 upregulation in azole-resistant clinical isolates of Candida albicans. Eukaryot Cell 11:1289-99.
23. Dunkel N, Liu TT, Barker KS, Homayouni R, Morschhäuser J, Rogers PD. 2008. A gain-of-function mutation in the transcription factor Upc2p causes upregulation of ergosterol

biosynthesis genes and increased fluconazole resistance in a clinical Candida albicans isolate. Eukaryot Cell 7:1180-90.

24. Whaley SG, Caudle KE, Vermitsky JP, Chadwick SG, Toner G, Barker KS, Gygax SE, Rogers PD. 2014. UPC2A is required for high-level azole antifungal resistance in Candida glabrata. Antimicrob Agents Chemother 58:4543-54.

25. Simonicova L, Moye-Rowley WS. 2020. Functional information from clinically-derived drug resistant forms of the Candida glabrata Pdr1 transcription factor. PLoS Genet 16:e1009005.

26. Hoot SJ, Smith AR, Brown RP, White TC. 2011. An A643V Amino Acid Substitution in Upc2p Contributes to Azole Resistance in Well-Characterized Clinical Isolates of Candida albicans. Antimicrobial Agents and Chemotherapy 55:940-942.

27. Heilmann CJ, Schneider S, Barker KS, Rogers PD, Morschhäuser J. 2010. An A643T Mutation in the Transcription Factor Upc2p Causes Constitutive ERG11 Upregulation and Increased Fluconazole Resistance in Candida albicans. Antimicrobial Agents and Chemotherapy 54:353-359.

28. Vermitsky JP, Edlind TD. 2004. Azole resistance in Candida glabrata: coordinate upregulation of multidrug transporters and evidence for a Pdr1-like transcription factor. Antimicrob Agents Chemother 48:3773-81.

29. Ferrari S, Ischer F, Calabrese D, Posteraro B, Sanguinetti M, Fadda G, Rohde B, Bauser C, Bader O, Sanglard D. 2009. Gain of function mutations in CgPDR1 of Candida glabrata not only mediate antifungal resistance but also enhance virulence. PLoS Pathog 5:e1000268.

30. Ni Q, Wang C, Tian Y, Dong D, Jiang C, Mao E, Peng Y. 2018. CgPDR1 gain-of-function mutations lead to azole-resistance and increased adhesion in clinical Candida glabrata strains. Mycoses 61:430-440.

31. Tsai H-F, Krol AA, Sarti KE, Bennett JE. 2006. Candida glabrata PDR1, a Transcriptional Regulator of a Pleiotropic Drug Resistance Network, Mediates Azole Resistance in Clinical Isolates and Petite Mutants. Antimicrobial Agents and Chemotherapy 50:1384-1392.

32. MacPherson S, Larochelle M, Turcotte B. 2006. A fungal family of transcriptional regulators: the zinc cluster proteins. Microbiol Mol Biol Rev 70:583-604.

33. Clarke M, Lohan AJ, Liu B, Lagkouvardos I, Roy S, Zafar N, Bertelli C, Schilde C, Kianianmomeni A, Bürglin TR, Frech C, Turcotte B, Kopec KO, Synnott JM, Choo C, Paponov I, Finkler A, Heng Tan CS, Hutchins AP, Weinmeier T, Rattei T, Chu JSC, Gimenez G, Irimia M, Rigden DJ, Fitzpatrick DA, Lorenzo-Morales J, Bateman A, Chiu C-H, Tang P, Hegemann P, Fromm H, Raoult D, Greub G, Miranda-Saavedra D, Chen N, Nash P, Ginger ML, Horn M, Schaap P, Caler L, Loftus BJ. 2013. Genome of Acanthamoeba castellanii highlights extensive lateral gene transfer and early evolution of tyrosine kinase signaling. Genome Biology 14:R11.

34. Klimova N, Yeung R, Kachurina N, Turcotte B. 2014. Phenotypic analysis of a family of transcriptional regulators, the zinc cluster proteins, in the human fungal pathogen Candida glabrata. G3 (Bethesda) 4:931-40.

35. Ollinger TL, Vu B, Murante D, Parker JE, Simonicova L, Doorley L, Stamnes MA, Kelly SL, Rogers PD, Moye-Rowley WS, Krysan DJ. 2021. Loss-of-Function ROX1 Mutations Suppress the Fluconazole Susceptibility of upc2AΔ Mutation in Candida glabrata, Implicating Additional Positive Regulators of Ergosterol Biosynthesis. mSphere 6:e0083021.

36. Vu BG, Stamnes MA, Li Y, Rogers PD, Moye-Rowley WS. 2021. The Candida glabrata Upc2A transcription factor is a global regulator of antifungal drug resistance pathways. PLoS Genet 17:e1009582.

37. Nagi M, Nakayama H, Tanabe K, Bard M, Aoyama T, Okano M, Higashi S, Ueno K, Chibana H, Niimi M, Yamagoe S, Umeyama T, Kajiwara S, Ohno H, Miyazaki Y. 2011.

Transcription factors CgUPC2A and CgUPC2B regulate ergosterol biosynthetic genes in Candida glabrata. Genes Cells 16:80-9.

38. Noble JA, Tsai HF, Suffis SD, Su Q, Myers TG, Bennett JE. 2013. STB5 is a negative regulator of azole resistance in Candida glabrata. Antimicrob Agents Chemother 57:959-67.

39. Pais P, Galocha M, Califórnia R, Viana R, Ola M, Okamoto M, Chibana H, Butler G, Teixeira MC. 2022. Characterization of the Candida glabrata Transcription Factor CgMar1: Role in Azole Susceptibility. J Fungi (Basel) 8.

40. Hickman MJ, Winston F. 2007. Heme Levels Switch the Function of Hap1 of Saccharomyces cerevisiae between Transcriptional Activator and Transcriptional Repressor. Molecular and Cellular Biology 27:7414-7424.

41. Davies BSJ, Rine J. 2006. A Role for Sterol Levels in Oxygen Sensing in Saccharomyces cerevisiae. Genetics 174:191-201.

42. Davies BSJ, Wang HS, Rine J. 2005. Dual Activators of the Sterol Biosynthetic Pathway of Saccharomyces cerevisiae: Similar Activation/Regulatory Domains but Different Response Mechanisms. Molecular and Cellular Biology 25:7375-7385.

43. Vik A, Rine J. 2001. Upc2p and Ecm22p, dual regulators of sterol biosynthesis in Saccharomyces cerevisiae. Mol Cell Biol 21:6395-405.

44. Tamura K-I, Gu Y, Wang Q, Yamada T, Ito K, Shimoi H. 2004. A hap1 mutation in a laboratory strain of Saccharomyces cerevisiae results in decreased expression of ergosterol-related genes and cellular ergosterol content compared to sake yeast. Journal of Bioscience and Bioengineering 98:159-166.

45. Marie C, Leyde S, White TC. 2008. Cytoplasmic localization of sterol transcription factors Upc2p and Ecm22p in S. cerevisiae. Fungal Genetics and Biology 45:1430-1438.

46. Barker KS, Pearson MM, Rogers PD. 2003. Identification of genes differentially expressed in association with reduced azole susceptibility in Saccharomyces cerevisiae. J Antimicrob Chemother 51:1131-40.

47. Giaever G, Nislow C. 2014. The yeast deletion collection: a decade of functional genomics. Genetics 197:451-65.

48. Takashima M, Sugita T. 2022. Taxonomy of Pathogenic Yeasts Candida, Cryptococcus, Malassezia, and Trichosporon Current Status, Future Perspectives, and Proposal for Transfer of Six Candida Species to the Genus Nakaseomyces. Medical Mycology Journal 63:119-132.

49. Shen X-X, Opulente DA, Kominek J, Zhou X, Steenwyk JL, Buh KV, Haase MAB, Wisecaver JH, Wang M, Doering DT, Boudouris JT, Schneider RM, Langdon QK, Ohkuma M, Endoh R, Takashima M, Manabe R-i, Čadež N, Libkind D, Rosa CA, DeVirgilio J, Hulfachor AB, Groenewald M, Kurtzman CP, Hittinger CT, Rokas A. 2018. Tempo and Mode of Genome Evolution in the Budding Yeast Subphylum. Cell 175:1533-1545.e20.

50. Steenwyk JL, Li Y, Zhou X, Shen X-X, Rokas A. 2023. Incongruence in the phylogenomics era. Nature Reviews Genetics 24:834-850.

51. Guarente L, Mason T. 1983. Heme regulates transcription of the CYC1 gene of S. cerevisiae via an upstream activation site. Cell 32:1279-86.

52. Fytlovich S, Gervais M, Agrimonti C, Guiard B. 1993. Evidence for an interaction between the CYP1(HAP1) activator and a cellular factor during heme-dependent transcriptional regulation in the yeast Saccharomyces cerevisiae. Embo j 12:1209-18.

53. Harbison CT, Gordon DB, Lee TI, Rinaldi NJ, Macisaac KD, Danford TW, Hannett NM, Tagne J-B, Reynolds DB, Yoo J, Jennings EG, Zeitlinger J, Pokholok DK, Kellis M, Rolfe PA, Takusagawa KT, Lander ES, Gifford DK, Fraenkel E, Young RA. 2004. Transcriptional regulatory code of a eukaryotic genome. Nature 431:99-104.

54. Gaisne M, Bécam AM, Verdière J, Herbert CJ. 1999. A 'natural' mutation in Saccharomyces cerevisiae strains derived from S288c affects the complex regulatory gene HAP1 (CYP1). Curr Genet 36:195-200.
55. Creusot F, Verdière J, Gaisne M, Slonimski PP. 1988. CYP1 (HAP1) regulator of oxygen-dependent gene expression in yeast. I. Overall organization of the protein sequence displays several novel structural domains. J Mol Biol 204:263-76.
56. Whaley SG, Zhang Q, Caudle KE, Rogers PD. 2018. Relative Contribution of the ABC Transporters Cdr1, Pdh1, and Snq2 to Azole Resistance in Candida glabrata. Antimicrob Agents Chemother 62.
57. Castanheira M, Deshpande LM, Davis AP, Carvalhaes CG, Pfaller MA. 2022. Azole resistance in Candida glabrata clinical isolates from global surveillance is associated with efflux overexpression. Journal of Global Antimicrobial Resistance 29:371-377.
58. Turi TG, Loper JC. 1992. Multiple regulatory elements control expression of the gene encoding the Saccharomyces cerevisiae cytochrome P450, lanosterol 14 alpha-demethylase (ERG11). Journal of Biological Chemistry 267:2046-2056.
59. Serratore ND, Baker KM, Macadlo LA, Gress AR, Powers BL, Atallah N, Westerhouse KM, Hall MC, Weake VM, Briggs SD. 2018. A Novel Sterol-Signaling Pathway Governs Azole Antifungal Drug Resistance and Hypoxic Gene Repression in Saccharomyces cerevisiae. Genetics 208:1037-1055.
60. Baker KM, Hoda S, Saha D, Gregor JB, Georgescu L, Serratore ND, Zhang Y, Cheng L, Lanman NA, Briggs SD. 2022. The Set1 Histone H3K4 Methyltransferase Contributes to Azole Susceptibility in a Species-Specific Manner by Differentially Altering the Expression of Drug Efflux Pumps and the Ergosterol Gene Pathway. Antimicrob Agents Chemother 66:e0225021.
61. Vu BG, Moye-Rowley WS. 2022. Azole-Resistant Alleles of ERG11 in Candida glabrata Trigger Activation of the Pdr1 and Upc2A Transcription Factors. Antimicrobial Agents and Chemotherapy 66:e02098-21.
62. Nakayama H, Tanabe K, Bard M, Hodgson W, Wu S, Takemori D, Aoyama T, Kumaraswami NS, Metzler L, Takano Y, Chibana H, Niimi M. 2007. The Candida glabrata putative sterol transporter gene CgAUS1 protects cells against azoles in the presence of serum. Journal of Antimicrobial Chemotherapy 60:1264-1272.
63. Zavrel M, Hoot SJ, White TC. 2013. Comparison of sterol import under aerobic and anaerobic conditions in three fungal species, Candida albicans, Candida glabrata, and Saccharomyces cerevisiae. Eukaryot Cell 12:725-38.
64. Li QQ, Tsai HF, Mandal A, Walker BA, Noble JA, Fukuda Y, Bennett JE. 2018. Sterol uptake and sterol biosynthesis act coordinately to mediate antifungal resistance in Candida glabrata under azole and hypoxic stress. Mol Med Rep 17:6585-6597.
65. Jordá T, Barba-Aliaga M, Rozès N, Alepuz P, Martínez-Pastor MT, Puig S. 2022. Transcriptional regulation of ergosterol biosynthesis genes in response to iron deficiency. Environ Microbiol 24:5248-5260.
66. Jordá T, Puig S. 2020. Regulation of Ergosterol Biosynthesis in Saccharomyces cerevisiae. Genes (Basel) 11.
67. Masoud GN, Li W. 2015. HIF-1α pathway: role, regulation and intervention for cancer therapy. Acta Pharm Sin B 5:378-89.
68. Fong GH, Takeda K. 2008. Role and regulation of prolyl hydroxylase domain proteins. Cell Death & Differentiation 15:635-641.
69. Gale AN, Sakhawala RM, Levitan A, Sharan R, Berman J, Timp W, Cunningham KW. 2020. Identification of Essential Genes and Fluconazole Susceptibility Genes in Candida glabrata by Profiling Hermes Transposon Insertions. G3 Genes|Genomes|Genetics 10:3859-3870.

70. Cowen LE, Sanglard D, Howard SJ, Rogers PD, Perlin DS. 2014. Mechanisms of Antifungal Drug Resistance. Cold Spring Harb Perspect Med 5:a019752.
71. Lee Y, Robbins N, Cowen LE. 2023. Molecular mechanisms governing antifungal drug resistance. npj Antimicrobials and Resistance 1:5.
72. Kitada K, Yamaguchi E, Arisawa M. 1995. Cloning of the Candida glabrata TRP1 and HIS3 genes, and construction of their disruptant strains by sequential integrative transformation. Gene 165:203-206.
73. Zordan RE, Ren Y, Pan SJ, Rotondo G, De Las Peñas A, Iluore J, Cormack BP. 2013. Expression plasmids for use in Candida glabrata. G3 (Bethesda) 3:1675-86.
74. Gregor JB, Gutierrez-Schultz VA, Hoda S, Baker KM, Saha D, Burghaze MG, Briggs SD. 2023. Expanding the toolkit for genetic manipulation and discovery in Candida species using a CRISPR ribonucleoprotein-based approach. bioRxiv doi:10.1101/2023.06.16.545382.
75. Yáñez-Carrillo P, Orta-Zavalza E, Gutiérrez-Escobedo G, Patrón-Soberano A, De Las Peñas A, Castaño I. 2015. Expression vectors for C-terminal fusions with fluorescent proteins and epitope tags in Candida glabrata. Fungal Genet Biol 80:43-52.
76. Grigoriev IV, Nordberg H, Shabalov I, Aerts A, Cantor M, Goodstein D, Kuo A, Minovitsky S, Nikitin R, Ohm RA, Otillar R, Poliakov A, Ratnere I, Riley R, Smirnova T, Rokhsar D, Dubchak I. 2011. The Genome Portal of the Department of Energy Joint Genome Institute. Nucleic Acids Research 40:D26-D32.
77. Skrzypek MS, Binkley J, Binkley G, Miyasato SR, Simison M, Sherlock G. 2017. The Candida Genome Database (CGD): incorporation of Assembly 22, systematic identifiers and visualization of high throughput sequencing data. Nucleic Acids Res 45:D592-d596.
78. Mersman DP, Du H-N, Fingerman IM, South PF, Briggs SD. 2012. Charge-based Interaction Conserved within Histone H3 Lysine 4 (H3K4) Methyltransferase Complexes Is Needed for Protein Stability, Histone Methylation, and Gene Expression*. Journal of Biological Chemistry 287:2652-2665.
79. Harmeyer KM, South PF, Bishop B, Ogas J, Briggs SD. 2015. Immediate chromatin immunoprecipitation and on-bead quantitative PCR analysis: a versatile and rapid ChIP procedure. Nucleic Acids Res 43:e38.
80. South PF, Harmeyer KM, Serratore ND, Briggs SD. 2013. H3K4 methyltransferase Set1 is involved in maintenance of ergosterol homeostasis and resistance to Brefeldin A. Proc Natl Acad Sci U S A 110:E1016-25.

FIGURE LEGENDS

FIG 1 Zinc cluster transcription factor Hap1 in *S. cerevisiae* alters fluconazole susceptibility. **(A and B)** Fluconazole susceptibility of BY4741, BY4741 *hap1Δ*, FY2609, and FY2611 *hap1Δ* of *S. cerevisiae* S288C strains. Five-fold serial dilution assays of indicated strains grown on SC plates with and without 16 μg/ml fluconazole and incubated at 30°C for 48 hr. **(C and D)** Growth curve of indicated strains grown in SC liquid media with or without 16 μg/ml fluconazole.

FIG 2 Evolutionary analysis of Hap1 homologs in fungi. **(A)** Species phylogeny showing the relationship of *C. albicans* and species within the *Saccharomycetaceae* (purple branches). Approximate divergence times of blue nodes are labeled. Location of the whole genome duplication event (WGD) is labeled. **(B)** Gene phylogeny of Hap1 homologs. The phylogeny was midpoint rooted and branch values represent ultrafast bootstrap support. Members of the *Saccharomycetaceae* are colored purple. Clades with more distantly related Hap1 homologs were collapsed for visualization (see Fig. S2 for the additional clades).

FIG 3 *C. glabrata* Zcf27, rather than, Zcf4 alters fluconazole susceptibility. **(A)** Five-fold serial dilution spot assays of *Cg*2001 WT, *zcf27Δ* and *zcf4Δ* strains plated on SC plates with and without 32 μg/mL fluconazole. **(B)** Liquid growth curves of the indicated *C. glabrata* strains grown in SC media with or without 32 μg/mL fluconazole. **(C)** Five-fold serial dilution assays of *Cg*989 WT and *zcf27Δ* transformed with plasmids expressing *ZCF27* from its endogenous promoter or empty vector spotted on SC-Ura plates with and without 32 μg/mL fluconazole at 30°C for 48 hr.

FIG 4 Transcript and protein analysis of *CYC1*, *ZCF27* and *ZCF4*. **(A and B)** Transcript levels of *CYC1* from the indicated strains treated with and without 64 μg/mL fluconazole for 3 hr. **(C and**

844 **D)** Transcript levels of *ZCF27* and *ZCF4* from the indicated strains treated with and without 64
845 µg/mL fluconazole for 3 hr. For A-D, transcript levels were set relative to WT and normalized to
846 *RDN18* mRNA levels. Data were analyzed from three or more biological replicates with three
847 technical replicates. Statistics were determined using the GraphPad Prism Student t-test,
848 version 9.5.1. Error bars represent SD. ns, P > 0.05; **P < 0.01. **(E)** Western blot analysis of
849 Zcf27-3X FLAG and Zcf4-3XFLAG with and without treatment with 64 µg/mL fluconazole for 3 hr
850 and 6 hr. Western blots showing short (Short Exp) and long (Long Exp) enhanced
851 chemiluminescence exposure. Histone H3 was used as the loading control.
852
853 **FIG 5** Transcript analysis of drug efflux pump and ergosterol (*ERG*) genes. **(A and B)** Transcript
854 levels of drug efflux pumps in *Cg*2001 WT and *zcf27Δ* strains treated with or without 64 µg/mL
855 fluconazole for 3 hr. **(C-F)** Transcript levels of *ERG* genes in *Cg*2001 WT and *zcf27Δ* strains
856 treated with or without 64 µg/mL fluconazole for 3 hr. For A-F, all strains were treated with or
857 without 64 µg/mL fluconazole for 3 hr. Transcript levels were set relative to the untreated WT
858 and normalized to *RDN18* mRNA levels. Data were analyzed from four biological replicates with
859 three technical replicates each. Statistics were determined using the GraphPad Prism Student t
860 test, version 9.5.1. ns, P > 0.05; *, P < 0.05; **, P <0.01. Error bars represent the SD.
861
862 **Fig 6** Chromatin immunoprecipitation analysis of Zcf27 at *ERG* gene promoters. **(A and B)**
863 ChIP analysis of *Cg*2001 WT (untagged) and Zcf27-3XFLAG at two *ERG11* promoter regions
864 (E11P1 and E11P2) when treated with or without 64 µg/mL fluconazole for 3 hr. **(C and D)** ChIP
865 analysis of Zcf27-3XFLAG at two *ERG3* promoter regions (E3P1 and E3P2) when treated with
866 and without 64 µg/mL fluconazole for 3 hr. For A-D, ChIP analysis was normalized to DNA input
867 samples and set relative to untagged WT. Statistics were determined using the GraphPad Prism
868 Student t test, version 9.5.1. ns, P > 0.05; *, P < 0.05; ***, P < 0.001; ****, P < 0.0001. Error bars
869 represent SD for three biological replicates with three technical replicates.

Fig 7 Disruption of ergosterol levels in a *zcf27Δ* strain alters azole susceptibility **(A-C)** HPLC analysis of the total ergosterol extracted from the *Cg*2001 WT and *zcf27Δ* strains treated with or without 64 µg/mL fluconazole for 3 hr. The figure represents a ratio between ergosterol and cholesterol, compared to treated and untreated WT samples. Data were generated from four biological replicates. Statistics were determined using the GraphPad Prism Student t test, version 9.5.1. ns, P > 0.05; *, P < 0.05. Error bars represent the SD. **(D and E)** Five-fold dilution spot assays of the indicated *C. glabrata* strains grown on SC plates with and without 32 µg/mL fluconazole and/or with and without 20 µg/mL ergosterol.

Fig 8 Phenotypic and expression analysis of *C. glabrata* strains under hypoxic conditions **(A)** Five-fold serial dilution spot assays of *Cg*2001 WT, *zcf27Δ* and *zcf4Δ* strains grown on YPD plates under aerobic and hypoxic condition. The fourth dilution of the hypoxic plate was enlarged for enhanced visibility **(B)** Graphical representation of colony sizes of the indicated strains when grown under hypoxic conditions. Colony sizes were measured using ImageJ, version 1.51. Statistics were determined using the GraphPad Prism Student t test, version 9.5.1. ns, P > 0.05; ***, P < 0.001. **(C and D)** Transcript analysis of *ZCF4* and *ZCF*27 of the *Cg*2001 WT strain when grown under hypoxic conditions over a time course of 0, 2, 4, 6, and 8 hrs. The relative transcript levels were set to *Cg*2001 WT before hypoxic exposure (0 hr) and normalized to *RDN18*. Statistics were determined using the GraphPad Prism Student t test, version 9.5.1. ns, P > 0.05; *, P < 0.05. **(E and F)** Western blot analysis of Zcf4-3XFLAG and Zcf27-3XFLAG protein levels over a time course of 0, 2, 4, 6, and 8 hr of hypoxic exposure. *Cg*2001 WT (untagged) strain was used as a negative control for both aerobic (Aer) and hypoxic (Hyp) conditions. Histone H3 was used as a loading control.

Fig 9 Ergosterol biosynthesis genes in *C. glabrata* are repressed upon hypoxic exposure. **(A-D)** The expression of *ERG11*, *ERG3*, *ERG2*, and *ERG5* was analyzed in *C. glabrata* WT cells

under both aerobic and hypoxic conditions. Transcript analysis was set relative to aerobic WT and normalized to *RDN18* as the internal control. Data were collected from a minimum of three biological replicates, each with three technical replicates. Statistics were determined using the GraphPad Prism Student t test, version 9.5.1. ns, P > 0.05; *, P < 0.05. Error bars represent the SD.

Fig 10 *ERG* genes are repressed by Zcf4 rather than Zcf27 upon hypoxic conditions. **(A-E)** After 8 hr of hypoxic exposure, transcript levels of *ERG11*, *ERG3*, *ERG5* and *ERG2* from the indicated strains were determined by qRT-PCR analysis. The levels of *ERG* genes were set relative to WT and normalized to *RDN18*. Data were generated from a minimum of three biological replicates. Statistics were determined using the GraphPad Prism Student t test, version 9.5.1. ns, P > 0.05; *, P < 0.05; **, P <0.01; ***, P < 0.001. Error bars represent the SD.

Fig 11 Chromatin immunoprecipitation analysis of Zcf27 and Zcf4 at *ERG* gene promoters under hypoxic conditions. **(A-H)** ChIP analysis of *Cg*2001 WT (untagged), Zcf27-3XFLAG and Zcf4-3XFLAG at two *ERG11* promoter regions (E11P1 and E11P2) and two *ERG3* promoter regions (E3P1 and E3P2) after 8 hr of hypoxic treatment. For A-H, ChIP analysis was normalized to DNA input samples and set relative to untagged WT. Data were generated from three biological replicates, with three technical replicates each. Statistics were determined using the GraphPad Prism Student t test, version 9.5.1. ns, P > 0.05; *, P < 0.05; **, P <0.01. Error bars represent the SD.

Fig 12 Model depicting the role of Zcf27 and Zcf4 in response to azole drug treatment and hypoxic conditions. **(A)** Under aerobic conditions with fluconazole treatment, Zcf27 (yellow) binds to the *ERG11* distal promoter region (E11P1), aiding in transcriptional activation of *ERG11*. Upc2A (green) binds to the *ERG11* proximal promoter region and is the commonly

known transcription factor for *ERG11*. Zcf4 is not depicted or control expression of *ERG11* because it is not expressed, as determined by our data, under these conditions. Under hypoxic conditions, Zcf4 is induced and highly expressed where it binds to the distal promoter sequence of *ERG11* to repress *ERG11* and to prevent binding of Zcf27. Zcf27 binds to the proximal promoter likely to prevent Upc2A binding. **(B)** Under aerobic conditions with fluconazole treatment, Zcf27 (yellow) binds to the *ERG3* distal promoter region (E3P1), aiding Upc2A in transcriptional activation of *ERG3*. Upc2A (green) is known to bind to the *ERG3* proximal promoter region and a known transcription factor for *ERG3*. Again, Zcf4 is not shown to control the expression of *ERG3* because it is not expressed. Under hypoxic conditions, Zcf4 is induced and highly expressed where it binds to the distal promoter and proximal promoter regions of *ERG3* to repress *ERG3* and to prevent binding of Zcf27 and likely Upc2A. Overall, this indicates utilization of three zinc cluster transcription factors for direct and distinct promoter control of *ERG* genes in response to azole treatment and hypoxic conditions. For A and B, arrows represent activation, while bars indicate inhibition. The dotted lines and question marks denote unknown interactions or regulatory mechanisms.

Figure 1:

A.

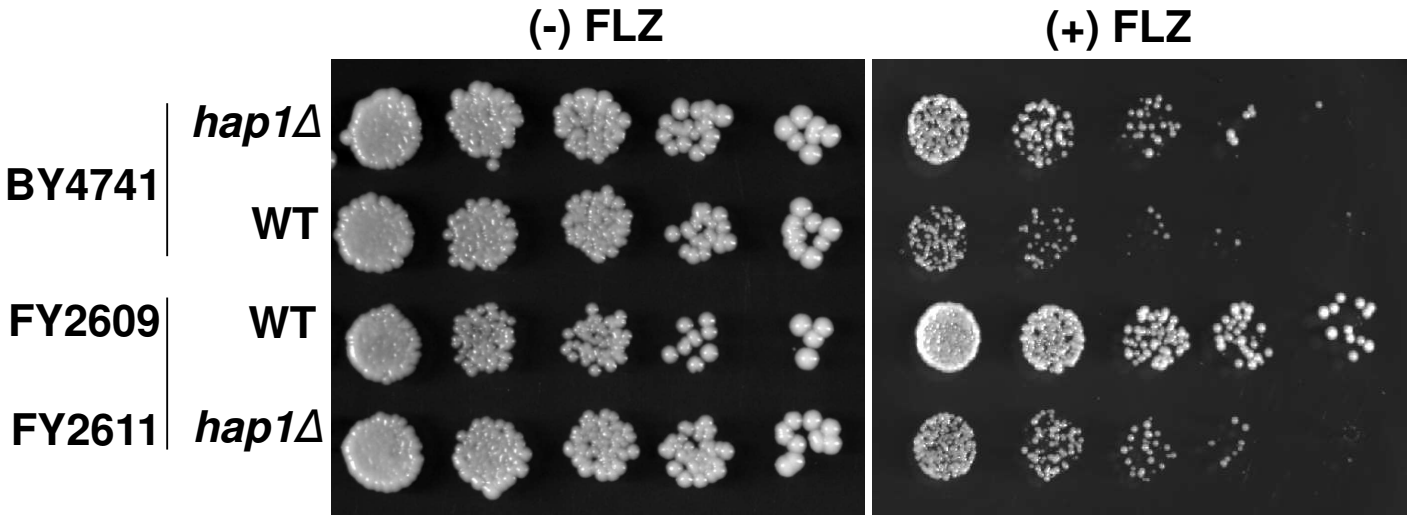

B.

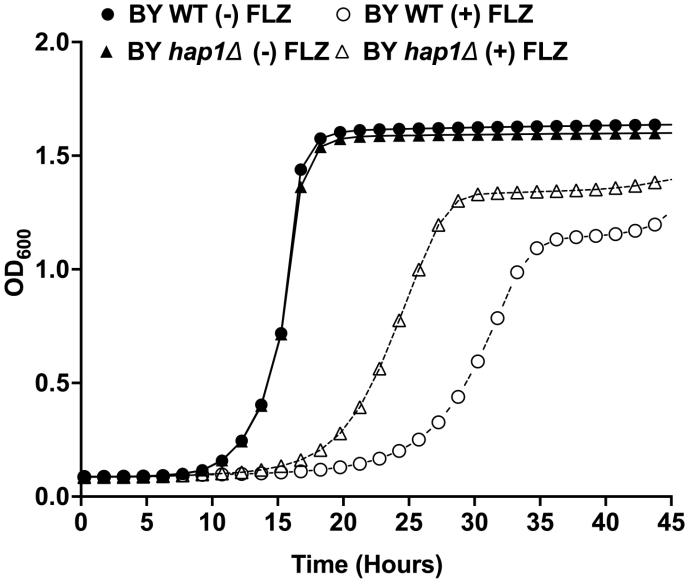

C.

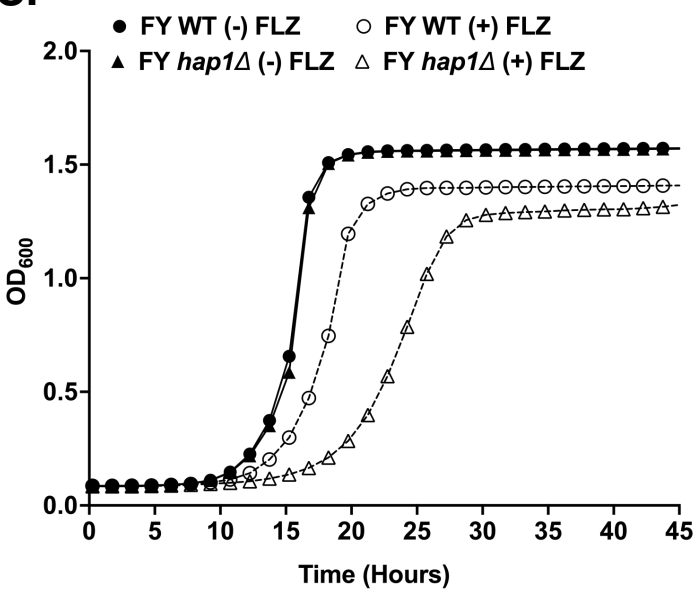

Figure 2:

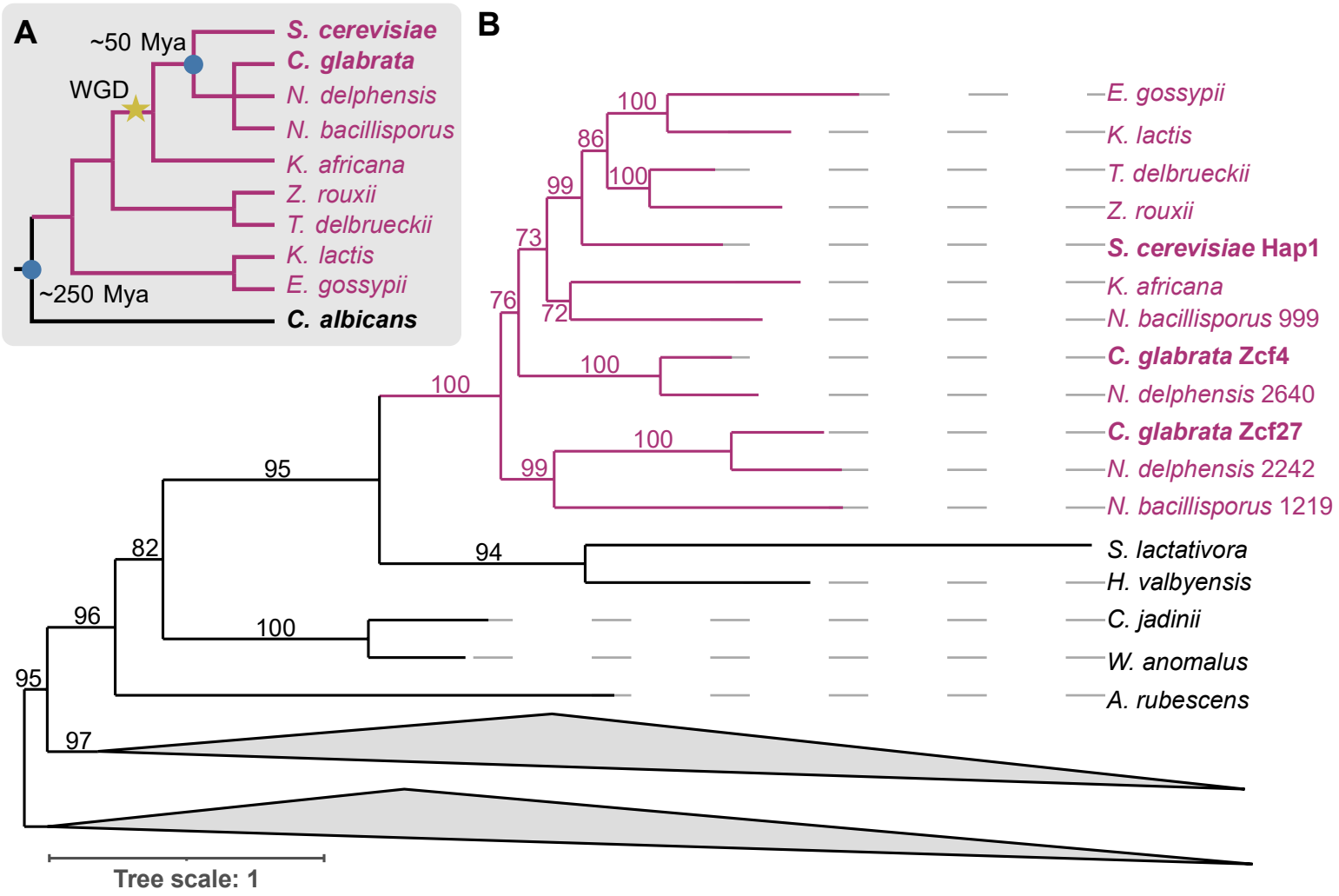

Figure 3:

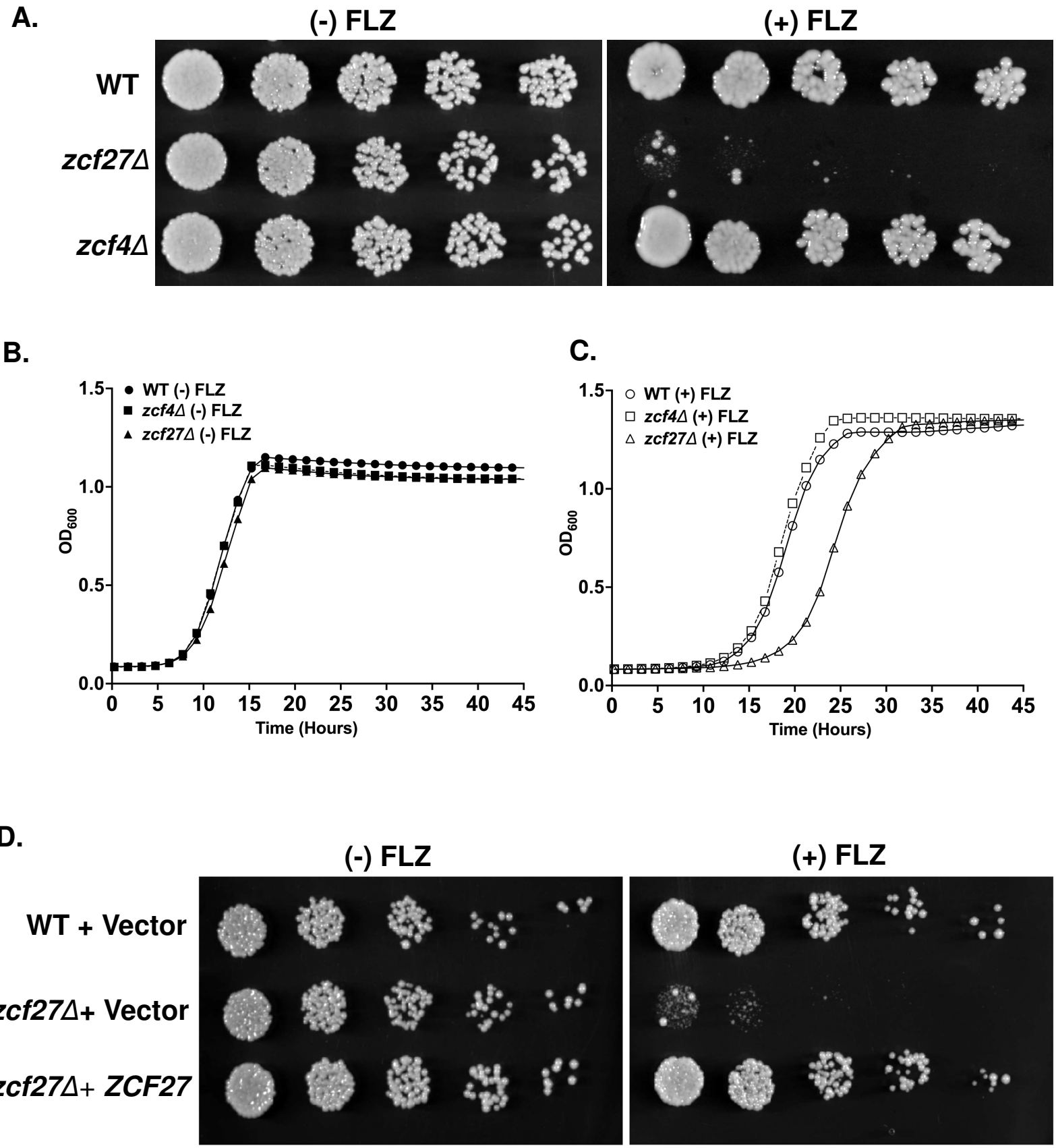

Figure 4:

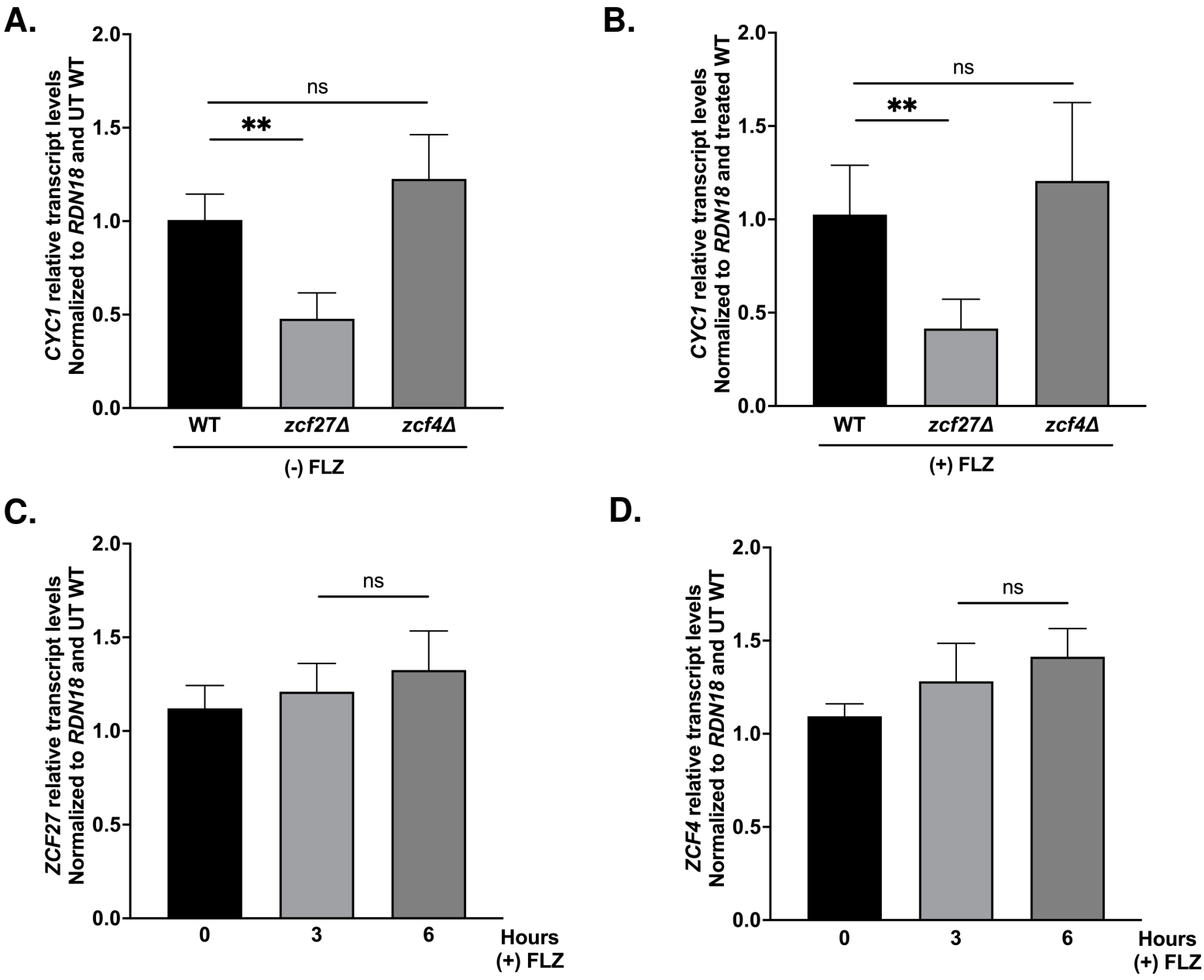

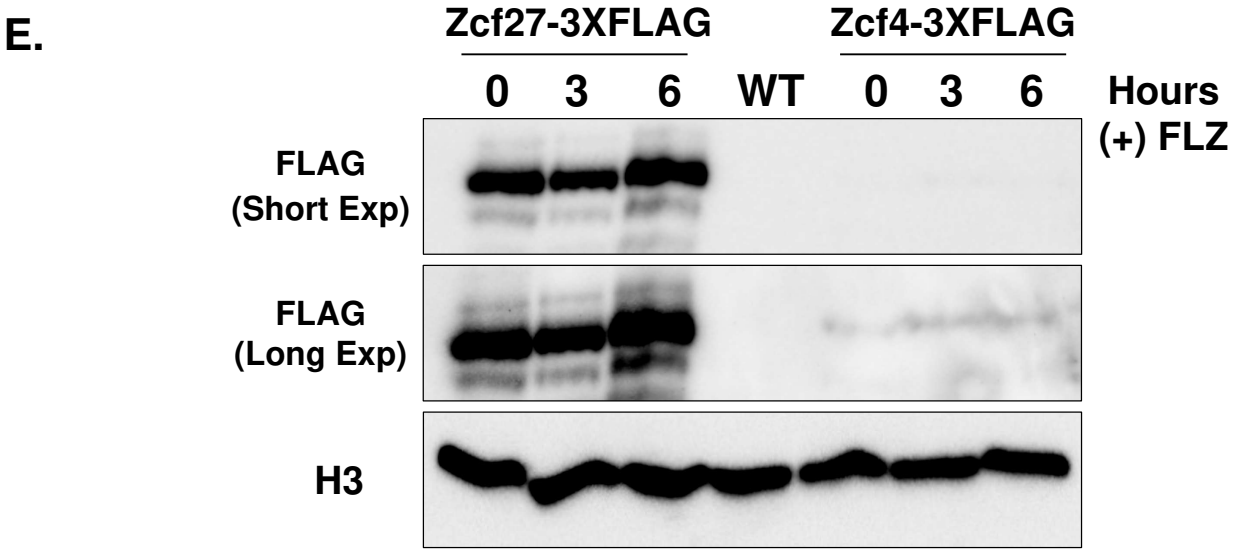

Figure 5:

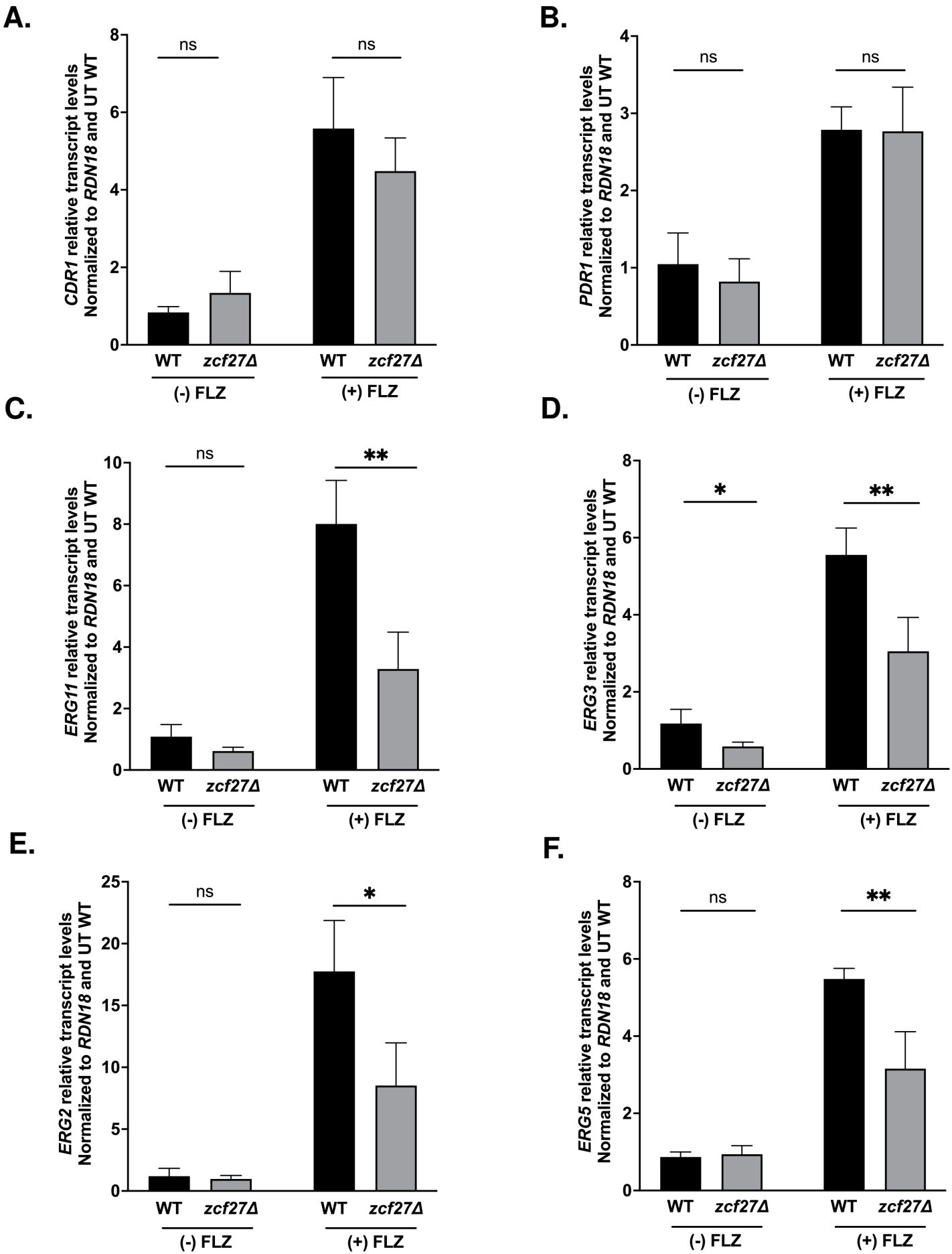

Figure 6:

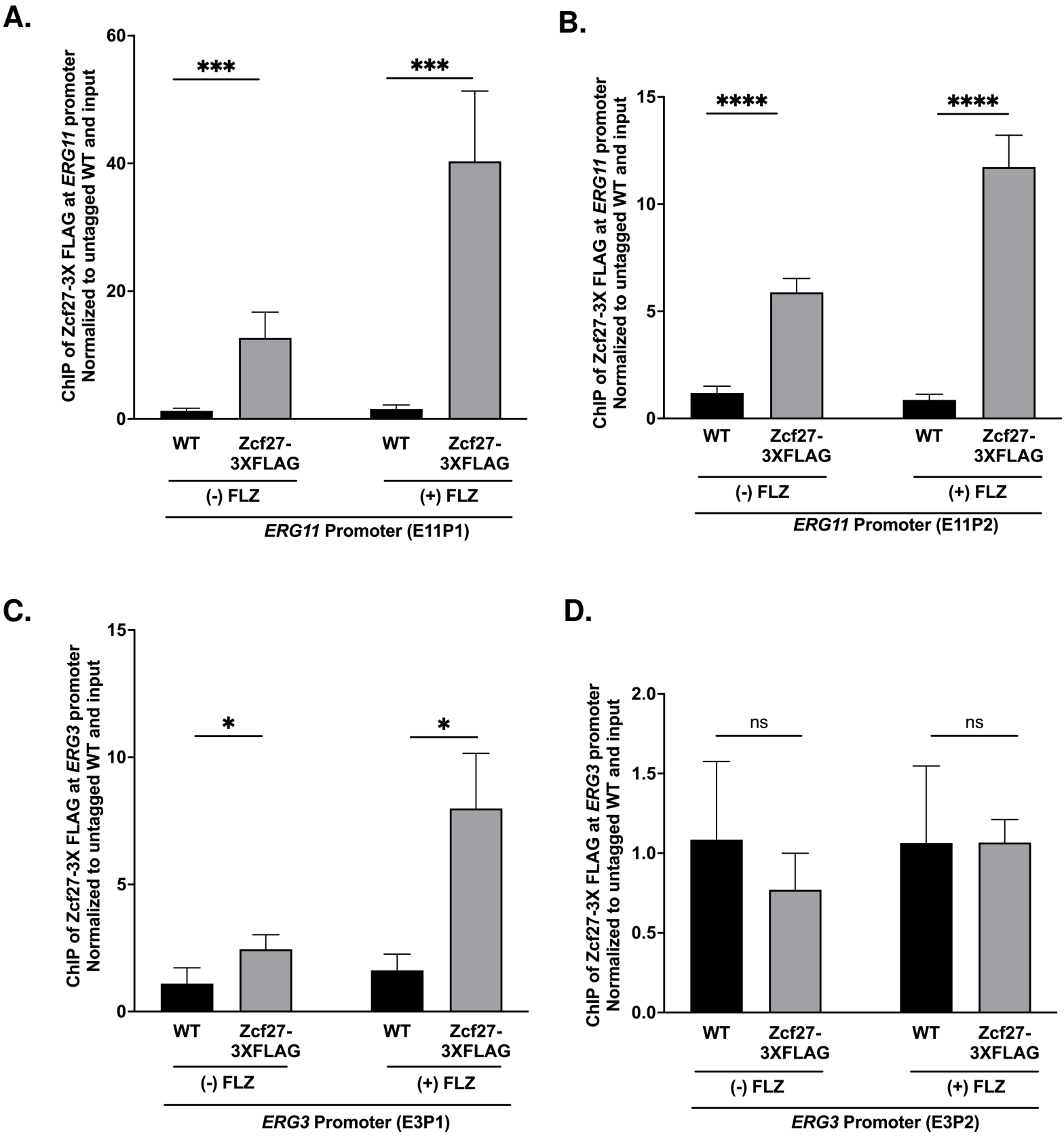

Figure 7:

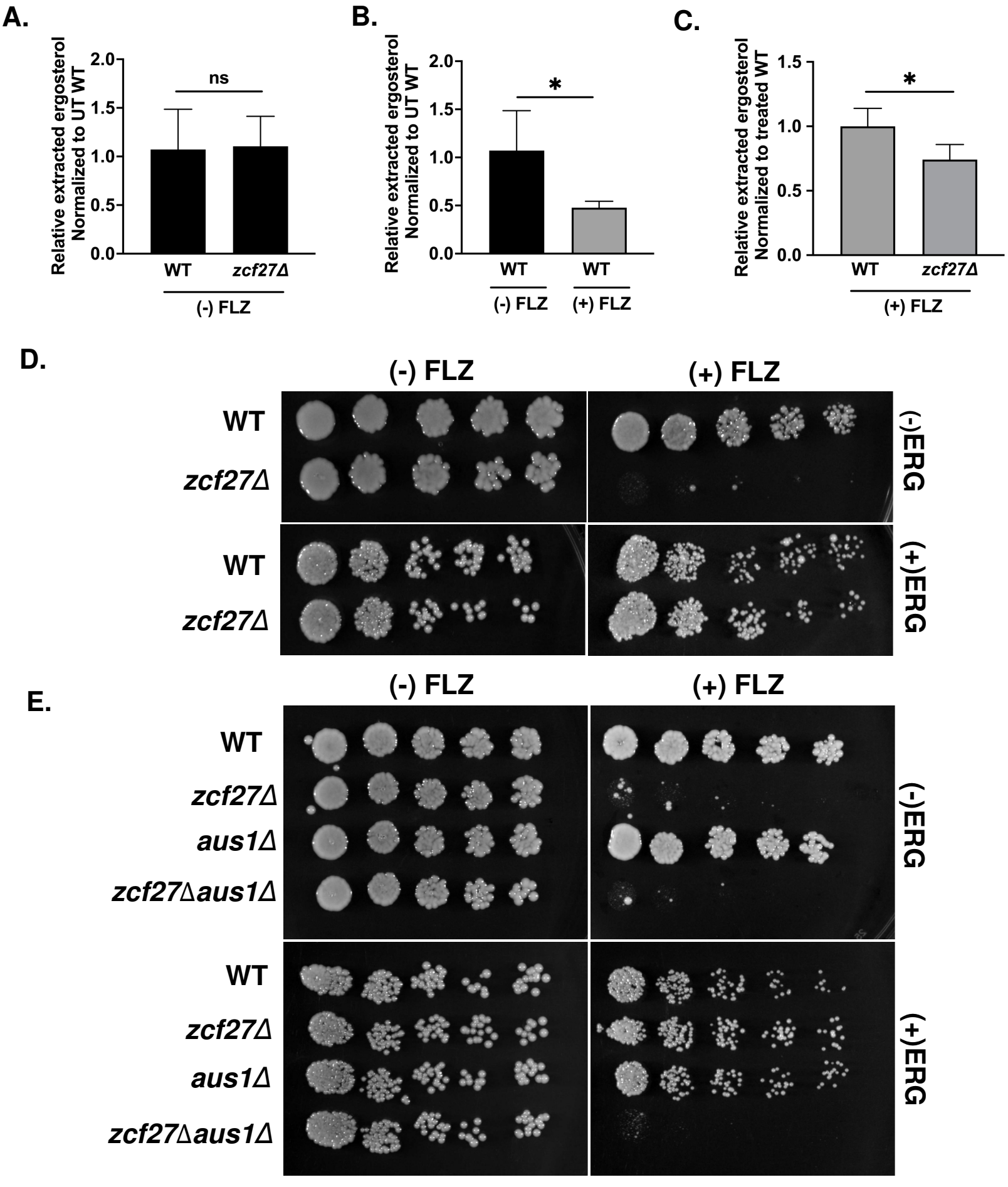

Figure 8:

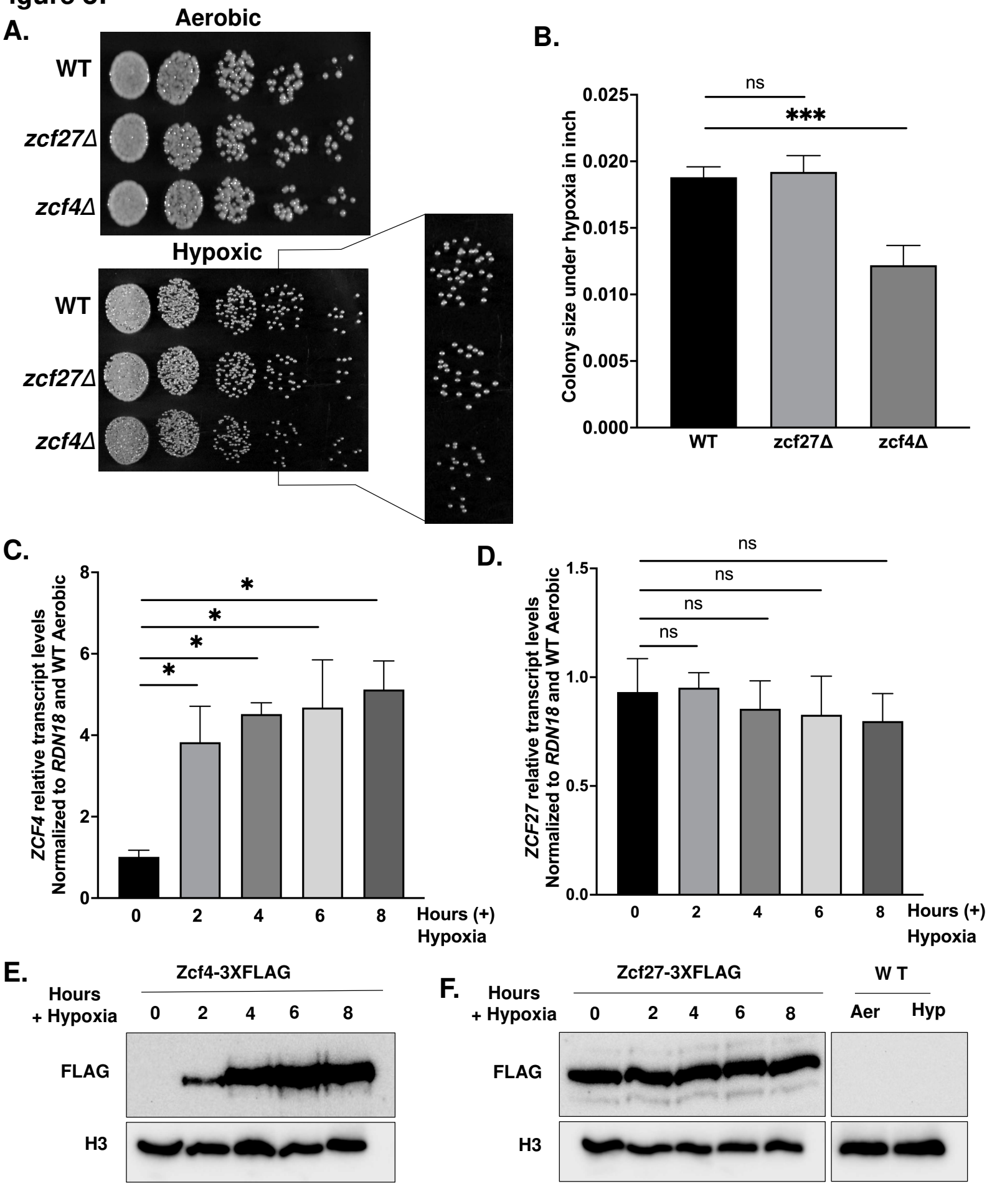

Figure 9:

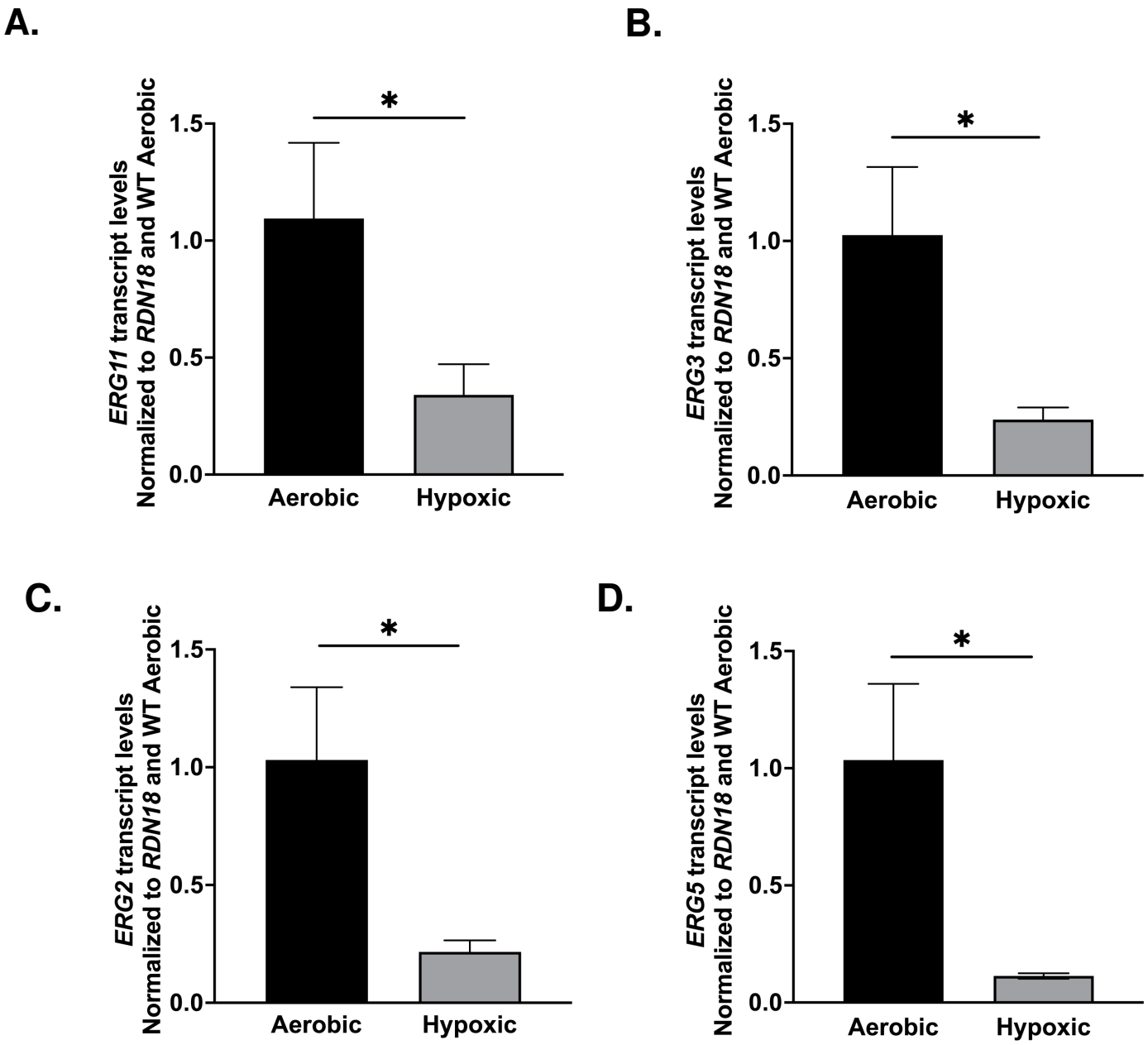

Figure 10:

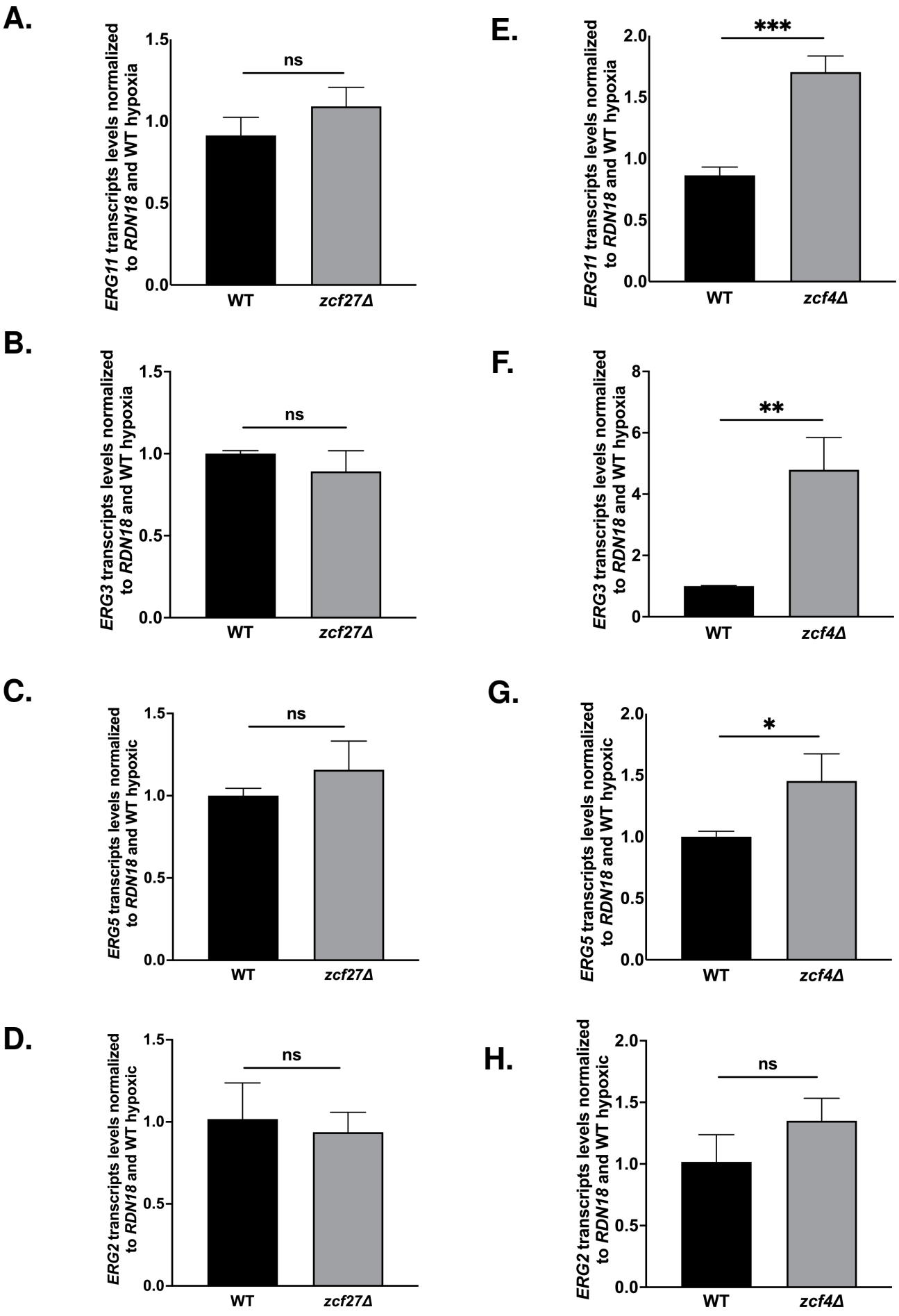

Figure 11:

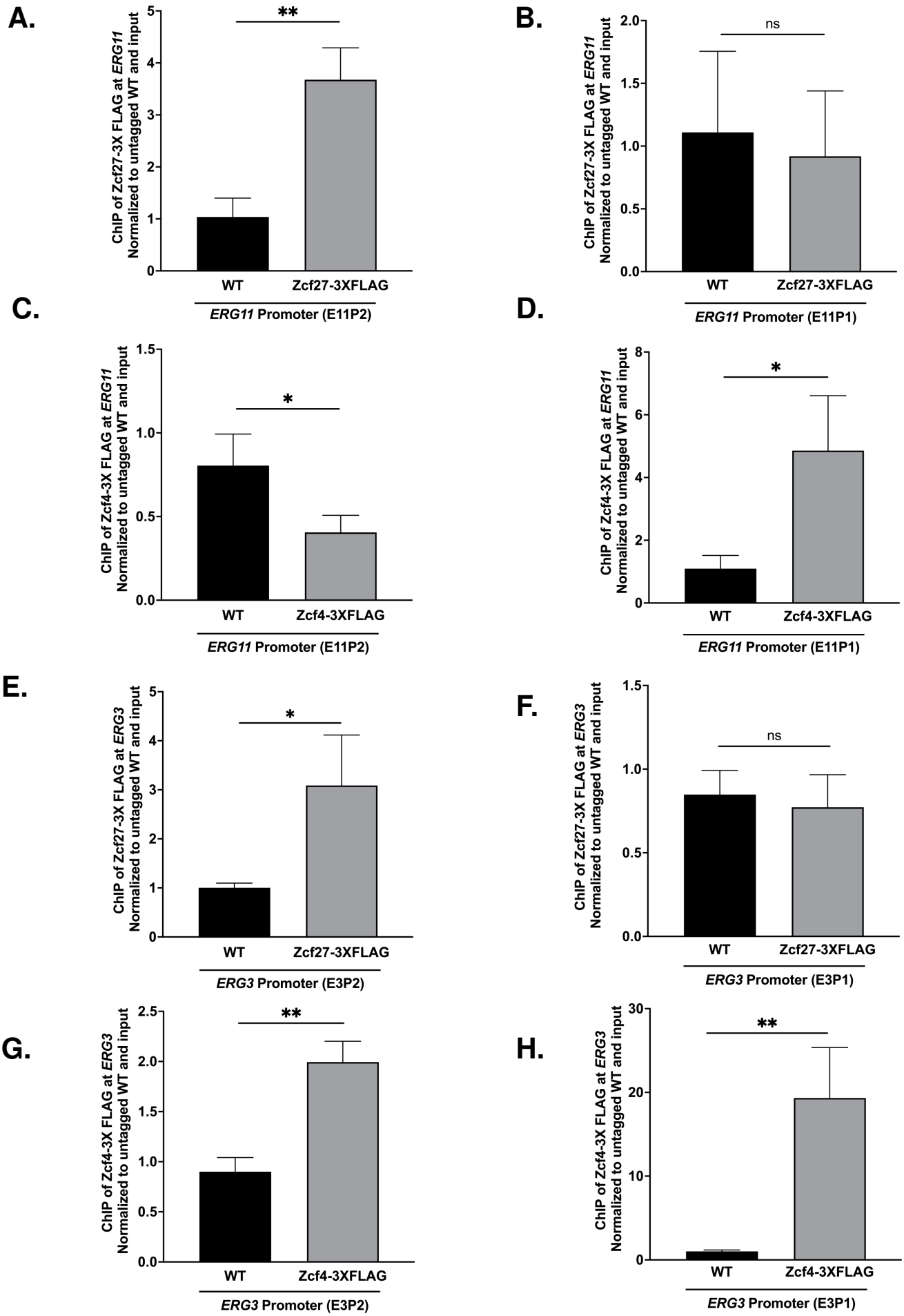

Figure 12: